LC-MS/MS METHOD DEVELOPMENT FOR QUANTITATION OF NICOTINE IN TOENAILS AS A BIOMAKER FOR SECONDHAND SMOKE AND STANDARD LIPOPROTEIN MIMETIC MODELS

A Dissertation

presented to

the Faculty of the Graduate School

at the University of Missouri-Columbia

In Partial Fulfillment

of the Requirements for the Degree

Doctor of Philosophy

---

by

XIYANG LI

Dr. C. Michael Greenlief, Dissertation Supervisor

December 2021

The undersigned, appointed by the dean of the Graduate School, have examined the dissertation entitled

LC-MS/MS METHOD DEVELOPMENT FOR QUANTITATION OF NICOTINE IN TOENAILS AS A BIOMAKER FOR SECONDHAND SMOKE AND STANDARD LIPOPROTEIN MIMETIC MODELS

presented by Xiyang Li,

a candidate for the degree of doctor of philosophy,

and hereby certify that, in their opinion, it is worthy of acceptance.

Professor C. Michael Greenlief

Professor Timothy E. Glass

Professor Lesa J. Beamer

Professor Chung-Ho Lin

ACKNOWLEDGEMENTS

I would like to thank my advisor, Dr. C. Michael Greenlief for all his mentoring and guidance during the past three years. Dr. Greenlief selected projects for me to work towards my career goal, and always shared lots of academic and industrial resources to give me opportunities to improve my instrumental performance and analysis skills. Dr. Greenlief's advice and guidance inspired me to figure out problems independently and become a more professional researcher in my future career path.

I would like to thank my parents for their support of me mentally and financially to begin my journey 10 years ago in the United States. Without their strong support and love, I could not make my life successful. My father and mother always offer whatever they have and never ask for anything in return. I also attribute my personal and work ethic to my parents for my life education and guidance.

My fiancée, Shuhan Zheng, always gives me her consistent love and support through my entire graduate school career. Her encouragement and kindness always bring me a positive vibe. I would not be able to reach the goals without her contributions.

In addition, I would like to give my thanks Dr. Renee D. JiJi and her research group members for my first two years of my graduate school for guidance and mentorship of my projects. With their help, I learned many things from the beginning of my graduate experience in her laboratory.

Finally, I would like to thank committee members Dr. Beamer, Dr. Glass, and Dr. Lin for their guidance and mentorship. I also thank the members of Dr. Greenlief research

group for their help and contributions. I would like to express my gratitude to the Department of Chemistry at the University of Missouri for providing me opportunities for my education.

TABLE OF CONTENTS

LIST OF FIGURES

LIST OF TABLES

LC-MS/MS METHOD DEVELOPMENT FOR QUANTITATION OF NICOTINE IN TOENAILS AS A BIOMRAKER FOR SECONDHAND SMOKE AND STANDARD LIPOPROTEIN MIMETIC MODELS

Xiyang Li

Dr. C. Michael Greenlief, Dissertation Supervisor

Abstract

Passive smoke or (secondhand smoke) is defined as when a non-smoker is unintentionally exposed to a smoking environment from cigarettes, cigars, or pipes. Passive smoke can result in adverse health effects leading to heart disease, asthma attacks, lung cancer, and other major diseases. Smoke from active smokers has been extensively investigated by a number of researchers. These studies have examined methods for the analysis of nicotine and its metabolites. In contrast, the development of methods to follow nicotine and its metabolites in those exposed to passive or secondhand smoke, is lacking. Here we present a method developed for the determination of nicotine in toenails. We will describe a method that involves the pretreatment of toenails, followed by a liquid-liquid extraction. The extract is then analyzed by reverse phase high performance liquid chromatography (HPLC) – ion trap mass spectrometry. Some of the figures of merit for this method include quantification of the nicotine concentration level, standard curve linearity ($R^2 > 0.99$), limit of detection (LOD = 0.005 ng/mg at m/z 163), and limit of quantitation (LOQ = 0.08 ng/mg), over the concentration range of 0.08 to 20 ng/mg. Toenail samples were individually collected for research purposes, including a non-smoker never exposed to secondhand smoke, non-smoker exposed to secondhand

smoke, and an active smoker. The results indicted mean of nicotine content in non-exposed, exposed, and active smoker toenails samples are 0.103, 0.415, and 1.75 ng/mg respectively. This study also compared a solid phase extraction method.

As a complex of globular proteins, lipoproteins, plays an essential role in the transport and metabolism of cholesterol. The level of several metabolites in blood are controlled by several mechanisms due to its profile. Development of common assays for lipoproteins have resulted in detection of abnormalities and can help physicians assess tissue injuries and disordering in early stages. Natural lipoprotein analysis related to cardiovascular disease is challenging even when utilizing modern analytical instrumentation. In this study, we developed mimetic lipoprotein models and characterize them using UV-Vis and fluorescence spectrophotometry to gain a better understanding of lipoproteins. An independent assay, the Amplex Red Cholesterol Assay, was also performed and used to support the mimetic lipoprotein model used in this study.

Cardiovascular health is associated with different classes of lipoproteins and the composition of each component in lipoproteins. This study demonstrated that the carbon-carbon double bond of cholesterol (1668 cm^{-1}) and the peptide backbone of tyrosine resonance are enhanced in deep ultraviolet resonance Raman (dUVRR) spectra (851, 1171, 1205, 1266, 1596, and 1615 cm^{-1}). The excitation of wavelength 197 nm characterized features of mimetic lipoprotein models. Other measurements, such as circular dichroism (CD), UV-vis, and fluorescence spectroscopy provided spectroscopic information to identity and characterize the mimetic lipoprotein models.

Chapter 1: Introduction

1.1 Tobacco

The word tobacco is derived from “tabaco” in Spanish and Portuguese. Tobacco was first discovered in ancient South America. Later on, tobacco was imported to Europe and cultivated in the 16th century. Originally when imported in Europe, tobacco was used as a cure for health problems. Cigarettes, a product of tobacco, became popular worldwide until it was shown to have negative health effects on humans.[1] To date, cigarettes are a heavily traded commodity and are still seen as a way of recreation. There is a significant amount of medical research about the effect of cigarettes in health issues such as cancer, cardiovascular disease, chronic obstructive pulmonary disease, miscarriage, and fetal underdevelopment.[2] Worldwide, consumption of tobacco causes about 7 million deaths pear year and predictions are that deaths may climb to 8 million per year by 2030 if regulation and control of tobacco does not change.[3,4] Smoking-related disease impacts over nearly 16 million Americans. Smoking can cause cancer, heart disease, stroke, lung disease, diabetes, and chronic obstructive pulmonary disease. More than 48,0000 deaths due to active smoking are reported each year in the United States. Moreover, the number of deaths per year due to secondhand smoke exposure is nearly 420,000.[5]

1.2 Nicotine

Nicotine is a natural alkaloid component of tobacco and represents approximately 3% of the total weight in tobacco. Nicotine was first isolated from *Nicotiana tabacum* in nightshade family. Red pepper, tomatoes, and potatoes are also in the nightshade family.[6] The nicotine structure, 3-[(2S)-1-methylpyrrolidin-2-yl]pyridine, is composed of two

nitrogen-containing heterocycles rings and is presented in Figure 1.1. Nicotine appears as a dark brown or pale yellow oil liquid. Nicotine is water soluble, but is light sensitive.[7]

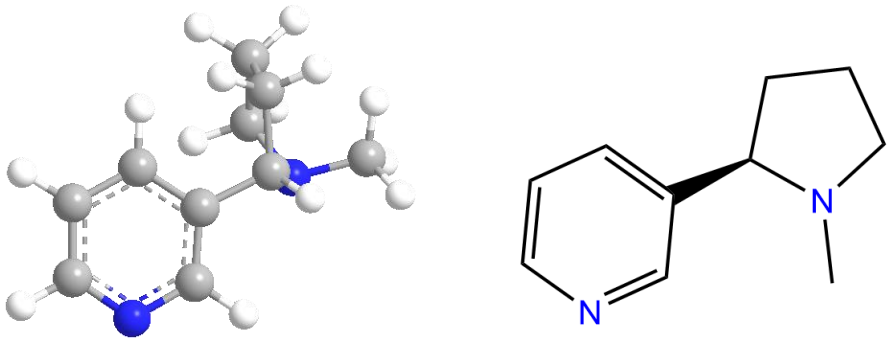

Figure 1. 1 Models of the nicotine structure.

1.3 Nicotine Absorption Pathways and Terminals

Dried tobacco blends with tar and nicotine is distilled from burning tobacco. It is then inhaled into the respiratory system. Alternatively, nicotine is easily absorbed into fabric or cloth and eventually enters human body fluids through skin exposure.[8,9] In human autopsy research, liver, kidney, spleen, brain, and lung are the highest affinity sites for nicotine. Nicotine also accumulates in gastric juice, saliva, and breast milk.[10,11] Typically, nicotine concentrations measured in blood range from 20 to 60 ng/mL and in urine are 1000 to 5000 ng/mL.[12,16] In addition, research indicates nicotine with can have a longer period of accumulation in keratic matrices, such as hair and toenails.[17,18]

1.4. Tobacco Exposure Related Diseases and Health Issues

1.4.1 Cancer

Nicotine can promote the formation of tumor cells. The cells are damaged, with suppressed cell function, and increase in proliferation and survival. Nicotine and its metabolite, cotinine, were discovered in studies about lung carcinogenesis. The antiapoptotic pathway was inhibited by nicotine and cotinine promoted lung tumorigenesis[19]. In addition, smokers with the CHRNA3 and CHRNA5 genes have higher carcinogenic nitrosamines and level of nicotine to induce lung cancer[20]. Liver DNA mutation occurred when the nicotine derivative, nitrosamine 4-(methylnitrosamino)-1-(3-pyridyl)-1-butanone (NNK), was involved and can result in gastro- intestinal carcinogenesis[21].

1.4.2 Cardiovascular Disease

Nicotine can cause the adrenal gland to release a monoamine neurotransmitter, catecholamine, that increases heart rate, hypertension, and cardiac contractility that eventually may lead to heart[22] malfunction. Atherosclerotic plaque formation resulted from nicotine alteration of vascular smooth muscle and endothelial cells in terms of their structure and functional characteristics[23].

1.4.3 Renal System

A high rate of chronic kidney disease was found in the smoking population. Studies of these smokers have found decreasing or failure of glomerular filtration rates that regulate

renal system detoxing, filtration, and acid-base balance. The end-stage of the chronic kidney disease will cause death[24].

1.4.4 Maternity

Low birth weight, spontaneous abortion, high infant mortality, and other childhood cognitive and learning problem are related to maternal smoking. Most studies have shown that tobacco alkaloids (nicotine, NNK, NNAL(4-(methylnitrosamino)-1-(3-pyridyl)-1-butanol)) were found in fetal urine, umbilical cord blood, and amniotic fluid[25].

1.5 Biomarker

1.5.1 Landmark of Biomarker in Clinical Research

In general, biomarkers serve as indicators for potential disease or the diagnosis of disease. Biomarkers are the result of biological processes, pathogenic processes, or pharmacologic responses. Biomarkers can be used for diagnostic purposes and are broadly applied for the evaluation and assessment of drug development or therapy.[26] In a noted study, it was discovered that increases in a glucose, insulin and homeostasis model assessment insulin resistance (HOMA-IR) were associated with cardiovascular disease in adults without diabetes.[27] Another example of a recent biomarker study by Courtney et al, reported changes in amyloid deposition as known as, β-amyloid 42 or Aβ-42, is a primary constituent of amyloid plaque, and increased levels of both total tau and hyperphosphorylated tau resulted in cognitive decline by measuring cerebrospinal fluid in normal middle aged health people. Based on their results, it was possible to predict the later risk of Alzheimer's disease.[28] Biomarkers greatly increase the values in clinical

research and clinical practice. Biomarkers have proven to be precise and specific in treatments in epidemiology.

1.5.2 Measurement of Biomarker of Tobacco Exposure

When nicotine enters the human body, it is processed and metabolized by liver enzymes. Nicotine and its metabolites are crucial to the understanding and assessing of tobacco exposure. Measurements of nicotine and its metabolites have provided significant support in smoke and non-smoke research. In modern analytical chemistry, quantitative analysis of nicotine and its metabolites are a growing area of research. Cutting-edge analytical instruments are more frequently used. These include, for example, gas chromatography, high performance liquid chromatography coupled with mass spectrometry or high resolution nuclear magnetic resonance (NMR) to study tobacco exposure to smokers and those exposed to secondhand smoke.

1.5.2.1 Blood

Nicotine concentrations were reported range from 5 to 30 ng/mL, with a mean of 10.9 ng/mL in human plasma. This measurement was determined by gas-chromatography-mass spectrometry (GC-MS). This study accessed the demographic, smoking status, and psychological predicator, along with nicotine concentration in human plasma.[29] Similarly, two other studies quantitatively measured nicotine and cotinine. The method involved simple liquid-liquid extraction from human plasma between non-smokers and smokers.[30,31] A comparative study of those exposed to secondhand smoke and smokers,

measured nicotine using radioimmunoassay (RIA) and enzyme-lined immunoassay (ELISA) to determine which methods are more efficient in epidemiological studies of human tobacco risks.[32]

1.5.2.2 Urine

Microextraction by packed sorbent (MEPS) methods were applied in the analysis of urine. The MEPS method uses a packing material similar to that used in solid phase extraction (SPE), but it often involves fewer steps and is relatively easy to perform compared to SPE. This study was limited by sample size, but the preparation methods and instrumentation used are worth considering.[33] Alternatively, a novel high-throughput LC-MS/MS can analyze more than 10 nicotine metabolites and nicotine in large population of urine sample in several proposed studies. The results of among these studies achieved high sensitivity and good reproducibility. Results revealed among measurements of both active smoke and secondhand smoke, measured levels of nicotine, cotinine and other metabolites are higher than other biological fluids that was considering a reliable evidence of relative accurate tobacco exposure, and its non-invasive collection more likely to be popular in these studies. In addition, with accurate level of nicotine, cotinine, and other metabolites can be measured by LC-MS/MS to target their role in lung cancer.[34,35,36,37,38,39,40,41]

1.5.2.3 Saliva

Saliva is the first body fluid to make contact with cigarette vapor as it enters the body. Vapor or gas phase constituents contain toxic chemicals including methanol, carbon

monoxide (CO), and other cigarettes derivative agents. High resolution ^{1}H-NMR detected the presence of methanol, propane-1,2-diol and other cigarettes derivative agents in collected human saliva. These results provided valuable information about the compounds that are unable be degraded in human saliva, as well as those that are oxidized in the mouth.[42] Thiocyanate can be used as a biomarker for tobacco smoke. It can be used to verify the smoking status during pregnancy and can be used to predict birth weight.[43,44] A study applied capillary electrophoresis (CE) methods to detect and quantitatively analyze thiocyanate in smokers' saliva. CE is able to handle large numbers of samples in support of clinical laboratories and provides valuable data in public health research.[45] Direct detection of nicotine is not readily done since nicotine has a short half-life time in saliva. Instead, salivary cotinine is mostly measured from secondhand smoke. A study group targeted smokers and those exposed to secondhand smoke and measured the concentrations of cotinine by HPLC-MS/MS to improve the precision and accuracy compared to CE. The study also found the potential of using cotinine as biomarker for optimizing pharmacotherapies for tobacco dependence.[46]

1.5.2.4 Hair

Analysis of hair from those exposed to secondhand smoke is popular in research. Nicotine, and its metabolites, have been measured in hair. The presence of these compounds could be followed for secondhand smoke exposure for up to at least 30 days. Easy sample preparation in the analysis resulted in reducing day to day variability. However, it requires more sensitive instruments to make the measurements. Liquid chromatography or gas chromatography are routinely used for nicotine and its

metabolites analysis. Some other approaches use LC/GC coupled ECD (high performance liquid chromatography electrochemical detector/gas chromatography electron capture detector) or MS to perform quantitative analysis. The sensitivity of the instrumental methods were reported with LODs between 0.02 ng to 0.2 ng nicotine/mg hair).[47,48,49,50] Nicotine concentrations were associated with race and hair color. The role melanin was found to be important as melanin has a high affinity to nicotine. Nicotine concentrations also depended on age. Younger children had higher concentration of nicotine compared to older children with the same secondhand smoke exposure.[51,52]

1.5.2.5 Toenails

Toenails are suitable for studying longer time exposures compared to hair. First, toenails grow slowly and reflect cumulative nicotine concentrations absorbed from blood circulation. Second, toenails were easily stored in ambient environments and are easy to collect. Wael et al studied toenail nicotine levels as a biomarker among smokers with and without lung cancer. They showed that the mean toenail nicotine level was 0.95 ng/mg of toenail in smokers with lung cancer. Interestingly, a statistical method (univariate and multivariate) analyzed highest versus lowest quintiles of toenail nicotine levels for smokers. In this study, the results predicted the risk for lung cancer based nicotine levels.[53] There a few studies that reported nicotine levels for those exposed to secondhand smoke using analytical methods including HPLC-ECD and GC-MS. The LODs varied from 0.025 to 0.1 ng/mg toenail.[54,55]

1.6 Plasma Lipoprotein

Plasma lipoproteins are macromolecules with complex particles. Phospholipids constitute the outer shell and cholesteryl ester and triglycerides are contained in the inner core. Free cholesterol and apolipoprotein bind on the lipoprotein surface and assemble to form a spherical like structure as shown in Figure 1.2. The primary role of lipoprotein is transportation. Since cholesterol and triglycerides are water insoluble, they are transported by lipoprotein. The secondary function is to transport toxic compounds, such as bacterial endotoxin. Transportation of triglycerides and cholesterol is important. Cells require cholesterol for steroidogenesis and triglycerides play a key component of metabolism.[57]

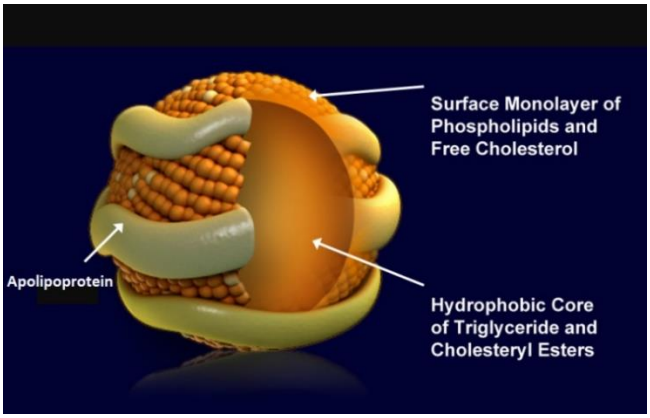

Figure 1.2 Lipoprotein Structure. Figure retrieved from The plasma lipoprotein: Structure and metabolism. Copyright©1978 by Annual Reviews, Inc.[56]

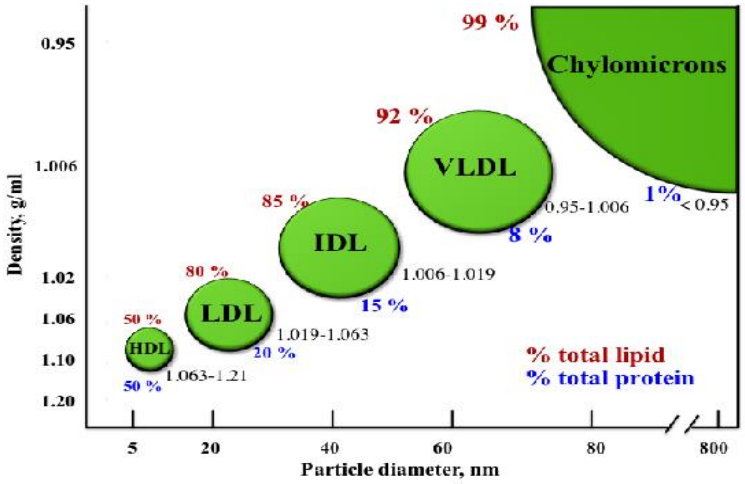

Figure 1.3 Lipoprotein Classifications. Figure retrieved from Study on the use of AFM to make traceable measurements of lipoprotein size distribution. Copyright© 2021 by IEEE[59]

Plasma lipoproteins are classified by particle size, lipid composition, and apolipoproteins as shown in Figure 1.3. Major classes of plasma lipoproteins are HDL (high density lipoproteins), LDL (low density lipoproteins), and VLDL (very low density lipoproteins). These different classes of lipoproteins have been studied in cardiovascular disease for decades.[58]

1.6.1 HDL-High Density Lipoprotein

HDL (high density lipoprotein) has the smallest size in the lipoprotein group. HDL carries excess cholesterol from peripheral tissue back to the liver, where it is removed from the body. The levels of HDL are inversely associated cardiovascular disease. HDL also plays functions in anti-inflammatory, anti-oxidant, and anti-atherogenic pathways.

Levels of HDL measured above 1.6 mmol/L indicated healthy individuals.[60,61] Analytical methods have studied HDL particles in terms of size and density. Most frequently, NMR and electrophoresis are used to make these measurements. Different sizes and densities of the HDL subunit are distinguished by type of apolipoproteins.[62,63] MALDI-TOF-MS/MS and LC-ESI-MS have been used to determine the compositions of HDL.[64,65]

1.6.2 LDL-Low Density Lipoprotein

Low density lipoproteins enrich cholesterol and carry the majority of cholesterol in body circulation. High levels of LDL resulted in higher risks of heart disease, obesity, type 2 diabetes and tissue infections. LDL also contains subunits based on their sizes and density. Smaller sized LDL retains a longer in arterial wall and eventually accrued cholesterol to block blood vessel, known as atherosclerosis.[66,67] The levels of LDL can be used to help evaluate the risk of heart disease. A precipitation and ultracentrifugation method was proposed to measure the concentration of apolipoprotein B in LDL to predict the risk of coronary disease.[68,69] In addition, a HPLC method provided a guideline to assess of the levels of LDL more accurately and avoid variations. This method used gel permeation chromatography to separate and identify the sizes of LDL and the results the study supported the need for further work on atherosclerosis.[70]

1.6.3 VLDL-Very Low Density Lipoprotein

VLDL is produced in the liver. VLDL mainly carries triglycerides and transfer triglycerides to tissues. The biggest difference between VLDL and LDL is the amount of cholesterol and triglycerides, in other words, LDL carries more cholesterols instead of

triglycerides. Similar to LDL, VLDL levels determine the risks of coronary artery disease and heart disease. Particularly, VLDL releases from the liver into the bloodstream and is eventually transformed into LDL. There are few assays to directly measured VLDL levels. Thus, triglycerides levels are measured and indirectly indicate the levels of VLDL. A recent study indicated a direct assessment level of VLDL by using an assay called mass sensitive sensor with molecularly imprinted polymers. This assay provided faster analysis of serum with less sample pre-treatment. The assay also had a good linear quantitative range and high sensitivity (limit of detection at 1.5 mg/dL).[71]

1.7 Biomimetic lipoproteins

The development of natural lipoproteins research has been impeded due to the low yield of lipoproteins in serum. Moreover, isolation of lipoproteins is challenging and requires high cost and sensitive instrumentation, such as size exclusion liquid chromatography,[72] HPLC-GPC (gel permeation column)[73] or gel electrophoresis.[74] Alternately, biomimetic lipoproteins have drawn attention in lipoprotein research. Researchers can synthesize lipoprotein particles in a mimetic model to provide feasibility of research in native lipoproteins and also can serve as targets in gene therapy, nucleic acid delivery, and cancer chemotherapy but not in cardiovascular treatment.[75,76 77] Recently, several studies have provided mimetic models of high density lipoproteins to reconstitute structures along with drug, combining in nanoparticles to target atherosclerosis treatments.[78]

1.8 Analytical Instrument Overview

1.8.1 HPLC-MS

High performance liquid chromatography (HPLC) is widely applied in small and large molecular separation, identification, and quantitation. HPLC have been an essential analytical technique in research and industry since it was first introduced in 1970. HPLC partitions targeted molecules by pressuring liquid solvent mixing with target samples through high pressure pumps. A column attached to an HPLC separates compounds by interactions with the column-packing material. The first 6000-psi HPLC devices were introduced 1972 with acronym HPLC-high pressure/high performance liquid chromatography. Since 1980, developing new methods and improving detection empower HPLC more rapidly and accurately.[79] HPLC coupled with mass spectrometry improves sensitivity and provided profiles and identification of each molecule. Mass spectrometry measures the mass to ratio (m/z) of ions. An ion trap mass spectrometer is a type of mass analyzer. Ions moved through a four symmetrically arrange electrodes that has a combined RF/DC voltage supplied as shown in Figure 1.4.

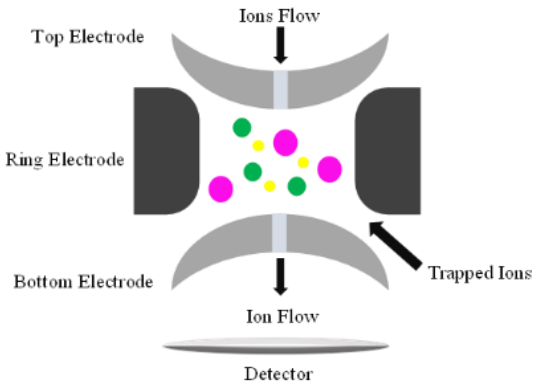

Figure 1.4 Representative ion trap schematic.[81]

Different m/z values can be transmitted to detector by changing the RF/DC voltage.[80] HPLC-MS is a combinatory analytical technique widely using in drug development, trace analysis, environmental analysis, and pharmaceutical research. With HPLC high specificity and robust handling complex mixtures, application of HPLC-MS in quantitative analysis will be discussed in next chapter.

1.8.2 dUVRRs-deep UV-Vis Resonance Raman Spectroscopy

The Raman effect is named after physicist C.V Raman. This effect describes an incident photon that interacts with a molecule resulting in an energy state transition. This process is initiated from vibrational states and molecules were excited creating photon scattering, and eventually relax back to the state with either less (stoke scattering) or greater (anti-stoke scattering) than original energy states as shown in Figure 1.5. This process causes energy lost in the photon and difference frequency of photon referred Raman scattering. The scattered frequencies were recorded as Raman shift, cm^{-1}. The excitation wavelength can be with UV light (λ_{exc}) is used to generate the signal intensity for Raman scattering. For an example, λ_{exc}=228 nm can generate a 500-fold stronger signal than at λ_{exc}=532 nm. Conventional Raman suffers from a fluorescence background that interferences in the analysis of many complex structures. Thus, a novel deep UV-Vis Resonance Raman spectroscopy (dUVRRs) was introduced avoid interference issues. Compared to conventional Raman, resonance Raman is able to coincide with electronic transitions, more specifically, information about the structure of molecules and properties accompanied with electronic transitioning. Furthermore, the deep UV-Vis (λ_{exc} < 210 nm)

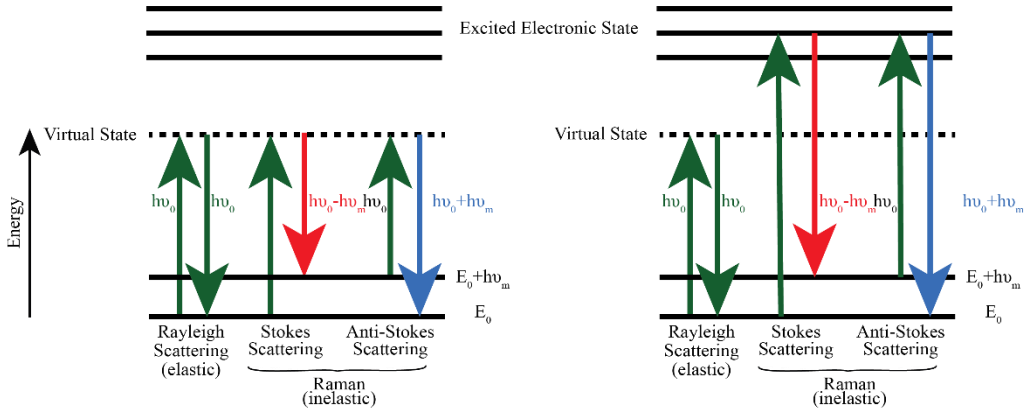

Figure 1. 5 Jablonski diagram of Raman scattering.[82]

enhanced Raman signal for some complex structure samples is very sensitive. dUVRRs has the advantage of selectivity since signal enhancement of Raman occurs only during electronic transitioning matched to the laser wavelength. Thus, this can be used to study particular molecules in complex samples.[83,84,85]

2. References

1. Goodman, Jordan. *Tobacco in History and Culture: An Encyclopedia*; Scribner turning points library; Thomson Gale: Detroit, 2005.
2. Action on Smoking and Health. Smoking Statistics: Who Smokes and How Much; ASH London, 2016.
3. World Health Organization. *WHO Report on the Global Tobacco Epidemic 2011*; World Health Organization: Geneva, 2011.
4. World Health Organization. *WHO Report on the Global Tobacco Epidemic, 2017external Icon*; World Health Organization: Geneva, 2017.
5. U.S. Department of Health and Human Services. *The Health Consequences of Smoking: 50 Years of Progress. A Report of the Surgeon General*; U.S. Department of Health and Human Services, Centers for Disease Control and Prevention, National Center for Chronic Disease Prevention and Health Promotion, Office on Smoking and Health: Atlanta, GA, 2014.
6. Fagerström, K. *J. Smok. Cessat.* **2014**, *9* (2), 53–59.
7. Crooks, P. A. Chapter 4 - Chemical Properties of Nicotine and Other Tobacco-Related Compounds. In *Analytical Determination of Nicotine and Related Compounds and their Metabolites*; Gorrod, J. W., Jacob, P., Eds.; Elsevier Science: Amsterdam, 1999; pp 69–147.
8. Gori, G. B.; Benowitz, N. L.; Lynch, C. J. *Pharmacol. Biochem. Behav.* **1986**, *25* (6), 1181–1184.
9. Noble, R. E. *Sci. Total Environ.* **2000**, *262* (1), 1–3.
10. Lindell, G.; Lunell, E.; Graffner, H. **1996**, *51* (3), 315–318.

11. Dempsey, D. A.; Benowitz, N. L. *Drug Saf.* **2001**, *24* (4), 277–322.

12. Feyerabend, C.; Higenbottam, T.; Russell, M. A. *Br. Med. J. Clin. Res. Ed* **1982**, *284* (6321), 1002–1004.

13. Gourlay, S. G.; Benowitz, N. L. *Clin. Pharmacol. Ther.* **1997**, *62* (4), 453–463.

14. Henningfield, J. E.; Keenan, R. M. *J. Consult. Clin. Psychol.* **1993**, *61* (5), 743–750.

15. Lunell, E.; Molander, L.; Ekberg, K.; Wahren, J. *Eur. J. Clin. Pharmacol.* **2000**, *55* (10), 737–741.

16. Rose, J. E.; Behm, F. M.; Westman, E. C.; Coleman, R. E. *Drug Alcohol Depend.* **1999**, *56* (2), 99–107.

17. Stepanov, I.; Hecht, S. S.; Lindgren, B.; Jacob, P.; Wilson, M.; Benowitz, N. L. R*Cancer Epidemiol. Biomark. Amp Prev.* **2007**, *16* (7), 1382.

18. Al-Delaimy, W. K.; Mahoney, G. N.; Speizer, F. E.; Willett, W. C. *Cancer Epidemiol. Biomark. Amp Prev.* **2002**, *11* (11), 1400.

19. Nakada, T.; Kiyotani, K.; Iwano, S.; Uno, T.; Yokohira, M.; Yamakawa, K.; Fujieda, M.; Saito, T.; Yamazaki, H.; Imaida, K.; Kamataki, T. *J. Toxicol. Sci.* **2012**, *37* (3), 555–563.

20. Le Marchand, L.; Derby, K. S.; Murphy, S. E.; Hecht, S. S.; Hatsukami, D.; Carmella, S. G.; Tiirikainen, M.; Wang, H. *Cancer Res.* **2008**, *68* (22), 9137.

21. Majidi, M.; Al-Wadei, H. A.; Takahashi, T.; Schuller, H. M. *Cancer Res.* **2007**, *67* (14), 6863.

22. Kaijser, L.; Berglund, B. *Clin. Physiol.* **1985**, *5* (6), 541–552.

23. Chalon, S.; Moreno Jr, H.; Benowitz, N. L.; Hoffman, B. B.; Blaschke, T. F. *Clin. Pharmacol. Ther.* **2000**, *67* (4), 391–397.

24. Jaimes, E. A.; Tian, R.-X.; Joshi, M. S.; Raij, L. *Am. J. Nephrol.* **2009**, *29* (4), 319–326.

25. Lackmann, G. M.; Salzberger, U.; Töllner, U.; Chen, M.; Carmella, S. G.; Hecht, S. S. Metabolites of a *JNCI J. Natl. Cancer Inst.* **1999**, *91* (5), 459–465.

26. World Health Organization; International Programme on Chemical Safety. Biomarkers and Risk Assessment : Concepts and Principles / Published under the Joint Sponsorship of the United Nations Environment Programme, the International Labour Organisation, and the World Health Organization. **1993**.

27. Gast, K. B.; Tjeerdema, N.; Stijnen, T.; Smit, J. W. A.; Dekkers, O. M. *PLOS ONE* **2012**, *7* (12), 1-8.

28. Sutphen, C. L.; Jasielec, M. S.; Shah, A. R.; Macy, E. M.; Xiong, C.; Vlassenko, A. G.; Benzinger, T. L. S.; Stoops, E. E. J.; Vanderstichele, H. M. J.; Brix, B.; Darby, H. D.; Vandijck, M. L. J.; Ladenson, J. H.; Morris, J. C.; Holtzman, D. M.; Fagan, A. M. *JAMA Neurol.* **2015**, *72* (9), 1029–1042.

29. Patterson, F.; Benowitz, N.; Shields, P.; Kaufmann, V.; Jepson, C.; Wileyto, P.; Kucharski, S.; Lerman, C. *Cancer Epidemiol. Biomark. Amp Prev.* **2003**, *12* (5), 468.

30. Shin, H.-S.; Kim, J.-G.; Shin, Y.-J.; Jee, S. H. *J. Chromatogr. B* **2002**, *769* (1), 177–183.

31. James, H.; Tizabi, Y.; Taylor, R. *J. Chromatogr. B. Biomed. Sci. App.* **1998**, *708* (1), 87–93.

32. Benkirane, S.; Nicolas, A.; Galteau, M.-M.; Siest, G. *Eur. J. Clin. Chem. Clin. Biochem.* **1991**, *29* (6), 405–410.

33. Iwai, M.; Ogawa, T.; Hattori, H.; Zaitsu, K.; Ishii, A.; Suzuki, O.; Seno, H. *Nagoya J. Med. Sci.* **2013**, *75* (3–4), 255–261.

34. Rangiah, K.; Hwang, W.-T.; Mesaros, C.; Vachani, A.; Blair, I. A. *Bioanalysis* **2011**, *3* (7), 745–761.

35. Heavner, D. L.; Richardson, J. D.; Morgan, W. T.; Ogden, M. W. *Biomed. Chromatogr.* **2005**, *19* (4), 312–328.

36. Piller, M.; Gilch, G.; Scherer, G.; Scherer, M. *J. Chromatogr. B* **2014**, *951–952*, 7–15.

37. Oh, J.; Park, M.-S.; Chun, M.-R.; Hwang, J. H.; Lee, J.-Y.; Jee, J. H.; Lee, S.-Y. *J. Anal. Toxicol.* **2020**, 1-12.

38. Stepanov, I.; Hecht, S. S.; Duca, G.; Mardari, I. *Cancer Epidemiol. Biomark. Amp Prev.* **2006**, *15* (1), 7.

39. Hecht, S. S.; Carmella, S. G.; Le, K.-A.; Murphy, S. E.; Boettcher, A. J.; Le, C.; Koopmeiners, J.; An, L.; Hennrikus, D. J. *Biomark. Amp Prev.* **2006**, *15* (5), 988.

40. Hecht, S. S.; Ye, M.; Carmella, S. G.; Fredrickson, A.; Adgate, J. L.; Greaves, I. A.; Church, T. R.; Ryan, A. D.; Mongin, S. J.; Sexton, K. *Cancer Epidemiol. Biomark. Amp Prev.* **2001**, *10* (11), 1109.

41. Hertsgaard, L. A.; Hanson, K.; Hecht, S. S.; Lindgren, B. R.; Luo, X.; Carmella, S. G.; Riley, W. T.; Zylla, E. B.; Murphy, S. E.; Hatsukami, D. K. *Cancer Epidemiol. Biomark. Amp Prev.* **2008**, *17* (12), 3337.

42. Percival, B.; Wann, A.; Masania, J.; Sinclair, J.; Sullo, N.; Grootveld, M. *JSM. Biotechnol. Bioeng.* **2018**, *5*(1), 1081.

43. Florescu, A.; Ferrence, R.; Einarson, T.; Selby, P.; Soldin, O.; Koren, G. *Ther. Drug Monit.* **2009**, *31* (1).

44. Hebel, J. R.; Fox, N. L.; Sexton, M. *J. Clin. Epidemiol.* **1988**, *41* (5), 483–489.

45. Phonchai, A.; Srisukpan, T.; Riengrojpitak, S.; Wilairat, P.; Chantiwas, R. *Anal. Methods* **2016**, *8* (25),

46. Jacob, P.; Yu, L.; Duan, M.; Ramos, L.; Yturralde, O.; Benowitz, N. L. *J. Chromatogr. B* **2011**, *879* (3), 267–276.

47. Mahoney, G.; Al-Delaimy, W. *J. Chromatogr. B. Biomed. Sci. App.* **2001**, *753*, 179–187.

48. Kim, S. R.; Wipfli, H.; Avila-Tang, E.; Samet, J. M.; Breysse, P. N. *Biomed. Chromatogr.* **2009**, *23* (3), 273–279.

49. Pichini, S.; Altieri, I.; Pellegrini, M.; Pacifici, R.; Zuccaro, P. *Proc. 1st Eur. Meet. Hair Anal. Clin. Occup. Forensic Appl.* **1997**, *84* (1), 243–252.

50. Zahlsen, K.; Nilsen, O. G. *Pharmacol. Toxicol.* **1994**, *75* (3–4), 143–149.

51. Kim, S.; Wipfli, H.; Navas-Acien, A.; Dominici, F.; Avila-Tang, E.; Onicescu, G.; Breysse, P.; Samet, J. M.; *Cancer Epidemiol. Biomark. Amp Prev.* **2009**, *18* (12), 3407.

52. Zahlsen, K.; Nilsen, T.; Nilsen, O. G. *Pharmacol. Toxicol.* **1996**, *79* (4), 183–190.

53. Al-Delaimy, W. K.; Willett, W. C. *Am. J. Epidemiol.* **2011**, *173* (7), 822–828.

54. Al-Delaimy, W. K.; Mahoney, G. N.; Speizer, F. E.; Willett, W. C. *Cancer Epidemiol. Biomark. Amp Prev.* **2002**, *11* (11), 1400.

55. Stepanov, I.; Feuer, R.; Jensen, J.; Hatsukami, D.; Hecht, S. S. *Cancer Epidemiol. Biomark. Amp Prev.* **2006**, *15* (12), 2378.

56. Smith, L. C.; Pownall, H. J.; Gotto, A. M. *Annu. Rev. Biochem.* **1978**, *47* (1), 751–777.

57. Rader, D. J. Lipoprotein Metabolism. In *Encyclopedia of Molecular Pharmacology*; Offermanns, S., Rosenthal, W., Eds.; Springer Berlin Heidelberg: Berlin, Heidelberg, 2008; pp 696–700.

58. Krauss, R. M. *Curr. Opin. Lipidol.* **2010**, *21* (4).

59. Demichelis, A.; Divieto, C.; Mortati, L.; Sassi, M.; Sassi, G. *2015 IEEE Int. Symp. Med. Meas. Appl. MeMeA Proc.* **2015**, 622–626.

60. Vergeer, M.; Holleboom, A. G.; Kastelein, J. J. P.; Kuivenhoven, J. Albert. T *J. Lipid Res.* **2010**, *51* (8), 2058–2073.

61. Barter, P.; Gotto, A. M.; LaRosa, J. C.; Maroni, J.; Szarek, M.; Grundy, S. M.; Kastelein, J. J. P.; Bittner, V.; Fruchart, J.-Charles. *N. Engl. J. Med.* **2007**, *357* (13), 1301–1310.

62. Jeyarajah, E. J.; Cromwell, W. C.; Otvos, J. D. *Atheroscler. Cardiovasc. Dis.* **2006**, *26* (4), 847–870.

63. Freeman, L. A. Native–Native 2D Gel Electrophoresis for HDL Subpopulation Analysis. In *Lipoproteins and Cardiovascular Disease: Methods and Protocols*; Freeman, L. A., Ed.; Humana Press: Totowa, NJ, 2013; pp 353–367.

64. Stuebiger, G.; Aldover-Macasaet, E.; Bicker, W.; Sobal, G.; Willfort-Ehringer, A.; Pock, K.; Bochkov, V.; Widhalm, K.; Belgacem, Omar. *Atheroscler. Amst. Neth.* **2012**, *224* (1), 177–186.

65. Koy, C.; Mikkat, S.; Raptakis, E.; Sutton, C.; Resch, M.; Tanaka, K.; Glocker, M. O. *Proteomics*. **2003**, *3* (6), 851–858.

66. Hevonoja, T.; Pentikäinen, M. O.; Hyvönen, M. T.; Kovanen, P. T.; Ala-Korpela, M. *Biochim. Biophys. Acta BBA - Mol. Cell Biol. Lipids* **2000**, *1488* (3), 189–210.

67. Lin, Jie. Low-Density Lipoprotein: Biochemical and Metabolic Characteristics and Its Pathogenic Mechanism. In *Apolipoproteins, Triglycerides Cholesterol*; IntechOpen Ltd: Rejika, 2020; pp 1–10.

68. Nauck, M.; Friedrich, I.; Wieland, H. *Comp. Ultracentrifugation Method Klin Lab* **1994**, *40*, 167–176.

69. Wieland, H.; Seidel, D. *J. Lipid Res.* **1983**, *24* (7), 904–909.

70. Usui, S.; Nakamura, M.; Jitsukata, K.; Nara, M.; Hosaki, S.; Okazaki, M. *Clin. Chem.* **2000**, *46* (1), 63–72.

71. Chunta, S.; Boonsriwong, W.; Wattanasin, P.; Naklua, W.; Lieberzeit, P. A. *Talanta* **2021**, *221*, 121549.

72. Busbee, D. L.; Payne, D. M.; Jasheway, D. W.; Carlisle, S.; Lacko, A. G. *Clin. Chem.* **1981**, *27* (12), 2052–2058.

73. Okada, T.; Ohama, T.; Okazaki, M.; Kanno, K.; Matsuda, H.; Sairyo, M.; Zhu, Y.; Saga, A.; Kobayashi, T.; Masuda, D.; Koseki, M.; Nishida, M.; Sakata, Y.; Yamashita, S. *PLOS ONE* **2018**, *13* (1), 1-13.

74. Li, Z.; McNamara, J. R.; Ordovas, J. M.; Schaefer, E. J. *J. Lipid Res.* **1994**, *35* (9), 1698–1711.

75. Baillie, G.; Owens, M. D.; Halbert, G. W. *J. Lipid Res.* **2002**, *43* (1), 69–73.

76. Hayavi, S.; Halbert, G. W. *Biotechnol. Prog.* **2005**, *21* (4), 1262–1268.

77. McMahon, K. M.; Mutharasan, R. K.; Tripathy, S.; Veliceasa, D.; Bobeica, M.; Shumaker, D. K.; Luthi, A. J.; Helfand, B. T.; Ardehali, H.; Mirkin, C. A.; Volpert, O.; Thaxton, C. S. *Nano Lett.* **2011**, *11* (3), 1208–1214.

78. Jiang, C.; Qi, Z.; Tang, Y.; Jia, H.; Li, Z.; Zhang, W.; Liu, Jianping. *Mol. Pharm.* **2019**, *16* (7), 3284–3291.

79. Robards, K.; Haddad, P. R.; Jackson, P. E. 5 - High-Performance Liquid Chromatography—Instrumentation and Techniques. In *Principles and Practice of Modern Chromatographic Methods*; Robards, K., Haddad, P. R., Jackson, P. E., Eds.; Academic Press: Boston, 2004; pp 227–303.

80. Wong, P. S.; Graham Cooks, R. *Curr. Sep.* **1997**, *16*, 85–92.

81. Diogo,R.D. A Short Overview of the Components in Mass Spectrometry Instrumentation for Proteomics Analyses. In *Tandem Mass Spectrometry*. IntechOpen: Rijeka, 2013; pp 40-57.

82. The Theory of Raman Spectroscopy. In *Modern Raman Spectroscopy – A Practical Approach.*; John Wiley & Sons, Ltd: Hoboken, NJ, 2004; pp 71–92.

83. López-Peña, I.; Leigh, B. S.; Schlamadinger, D. E.; Kim, J. E. *Biochemistry* **2015**, *54* (31), 4770–4783.

84. Merlin, J. C. *Pure Appl. Chem.* **1985**, *57* (5), 785–792.

85. Johnson, B. B.; Peticolas, W. L. *Annu. Rev. Phys. Chem.* **1976**, *27* (1), 465–521.

Chapter 2: LC-MS/MS Method Development for Quantitation of Nicotine in Toenails as a Biomarker for Secondhand Smoke

2.1 Introduction

In general, active tobacco smoking can lead to cancer and cardiovascular disease.[1,2] Secondhand smoke, also known as environmental tobacco smoke, has been classified as a class A carcinogen, and is implicated in the same diseases as active tobacco smoking.[3] A report published about people exposed to secondhand smoke showed that there was a higher risk of lung cancer (about 1.3-fold) compared to people not exposed to secondhand smoke. Biomarkers play important roles of identification of human disease. They can be found in blood, urine, body fluid, and tissue samples. Nicotine acts as a biomarker of exposure to smoking environments and is crucial in understanding mechanisms for human disease. Measurements of nicotine concentrations in body fluids, such as blood and saliva, are also commonly used by clinical researchers to understand both active smokers and people exposed to secondhand smoke connecting to its role in disease.[4,5] One of tobacco's main components is nicotine. Nicotine is easily absorbed by humans and can be detected in blood, serum, and other body fluids. This project is targeting the analysis of nicotine concentration in toenails. Less contamination from external sources, slow growth, easy collection and storge make toenails a popular choice in forensic and clinical studies. Additionally, analytes in toenails can be attributed to cumulative exposure over a longer period, specifically to studies of chronic disease.[6,7]

A previous study of human toenails for the presence of nicotine was reported by Irina.[8] This study quantitatively measured the nicotine content from secondhand smoke in human toenails by applying GC-MS. However, this GC-MS method gave quantitation

limits with high background noise.[8] Another study of nicotine content in human hair was reported by Mahoney.[9] This study used HPLC-ED (high performance liquid chromatography with electrochemical detection). Even though this instrumental method used HPLC-ED, decreased selectivity resulted in increased background noise. Recent quantitative analysis of hair for nicotine content has improved its quantitation limits and selectivity by using liquid chromatography-mass spectrometry (LC-MS).[10-12] However, studies examining the use of study human toenails exposed to secondhand smoke with using HPLC-MS are lacking.

In this study, we describe the development of a method to measure quantitatively the concentration of nicotine in human toenails. High performance liquid chromatography and ion trap mass spectrometry are applied to investigate the nicotine concentration levels in toenails from individuals exposed to secondhand smoke. High performance liquid chromatography, equipped with C_{18} reverse phase column to provide robustness of separation, less time analysis, good peak shape, coupled with electron spray ionization mass spectrometry can provide a quantitative, highly selective and sensitive method for analysis.[13]

2.2 Materials and Methods

2.2.1 Chemicals

Analytical grade nicotine was purchased from Sigma-Aldrich. The internal standard nicotine-d_3 ((±)-nicotine-d_3 in ethanol) was purchased from Cayman Chemical.

Methylene chloride, isopropyl, and diethyl ether used for extractions were purchased from Fisher Scientific (Hampton, NH). All solvents were HPLC grade or ACS certified.

2.2.2 Standard and Sample Preparation

A stock solution of 10 mg/L of nicotine and a solution of 1 mg/L of the internal standard were prepared in 0.01 % formic acid in 80:20 H_2O/ACN (v/v). Standard solutions were prepared by serial dilution. 100 µL of a nicotine standard and 50 µL of the internal standard were added to the low nicotine toenail digest (no exposure to secondhand smoke) before extraction. Calibration curves covered the range from 8 to 2000 pg/mg for the spiked samples. The calibration curve was then used to aid in the quantitation of the unknowns. Samples were collected from volunteers who were friends of the author for quality control and sample analysis. The samples were clipped from 10 toes and 10 to 30 mg of toenails were enough for purpose of analysis. Sample preparation and analysis in this research were similar to a previous study of hair samples.[9] The sample preparation steps involved washing with dichloromethane (90 min), digestion at 50°C overnight in 1 M of NaOH, and then a liquid-liquid extraction was performed with diethyl ether. The obtained organic phase was dried under nitrogen at 35°C. The methodology agreed with a previous study that reported no difference in results when using air or nitrogen for evaporating the diethyl ether, so a nitrogen stream was used to dry all extractions.[9] Furthermore, the addition of 0.01% HCl in methanol in ether layer increased the stability of the chloride salt of nicotine without loss of nicotine content.[16] The dried residue was redissolved in 100 µL of the HPLC mobile phase and transferred to HPLC autosampler vials with polypropylene inserts. The injection volume for the HPLC was 5 µL.

2.2.3 HPLC Conditions

The HPLC-MS analysis were performed using Perkin Elmer series 200 HPLC system coupled to a ThermoFinnigan LCQ-Deca XP plus ion trap. A reversed phase C_{18} column (5 µm particle size, 2 mm × 150 mm, Phenomenex) was used and held at 30°C. The mobile phase consisted of 80% (A) water and 20% (B) acetonitrile both in 0.1% formic acid. The flow rate was 0.2 mL/min and the isocratic elution was run for 5 min.

2.2.4 MS Detector

The mass spectrometer was operated in the positive-ion mode. The electrospray ionization (ESI) source used an ion-spray voltage of 4.3 kV. Nitrogen gas was used as the auxiliary and sheath gases with a flow rate of 20 L/min and 45 L/min, respectively. A 500 µL Hamilton syringe (Reno, NV) was used in the ESI-MS syringe pump and flow rate was set up to 200 µL/min to performed direct injection analysis. Helium gas was used for collision induced dissociation (CID) of ions. The collision energy was set to 31%. The capillary temperature was set to 225°C and capillary voltage was 3.0 V. The maximum inject time was 200.03 ms and the total number of microscans was set to three.

2.3 Results and Discussion

2.3.1 HPLC-MS

Nicotine (analytical grade standard) was used in the quantification of nicotine levels in toenails for this study. Sample preparation in this research was similar to a previous study

of hair samples.[9] ESI-MS direct injection were firstly performed to identify nicotine and nicotine-d_3 in mass spectra. Mass spectrometry analysis of nicotine gave a protonated molecule, $[M+H]^+$, at m/z 163 Da (Figure 2.1). Applied collision energy described in methods and material section and generated two major fragmentation ions were observed at m/z 132 and m/z 106 Da. The fragment ion with the loss of 31 Da (from the parent ion) was due to the methylamine group from the heterocyclic ring and loss of 57 Da was due to N-methylamine from pyrrolidine ring, as seen in Figure 2.1. Similar to the nicotine standard, nicotine-d_3 was selected for the internal standard. The MS/MS spectrum of nicotine-d_3 (Figure 2.2) showed has similar molecular weight to nicotine and identical fragmentation ions, these features give precision in quantitative analysis. The purpose of performing direct injection in ESI-MS to applied tuned mass spectral signal in accordance with HPLC-MS. In addition, nicotine-d_3 has the advantage of allowing for the correction of matrix effects and co-elutes with analyte, but is easily distinguished by mass spectrometry.

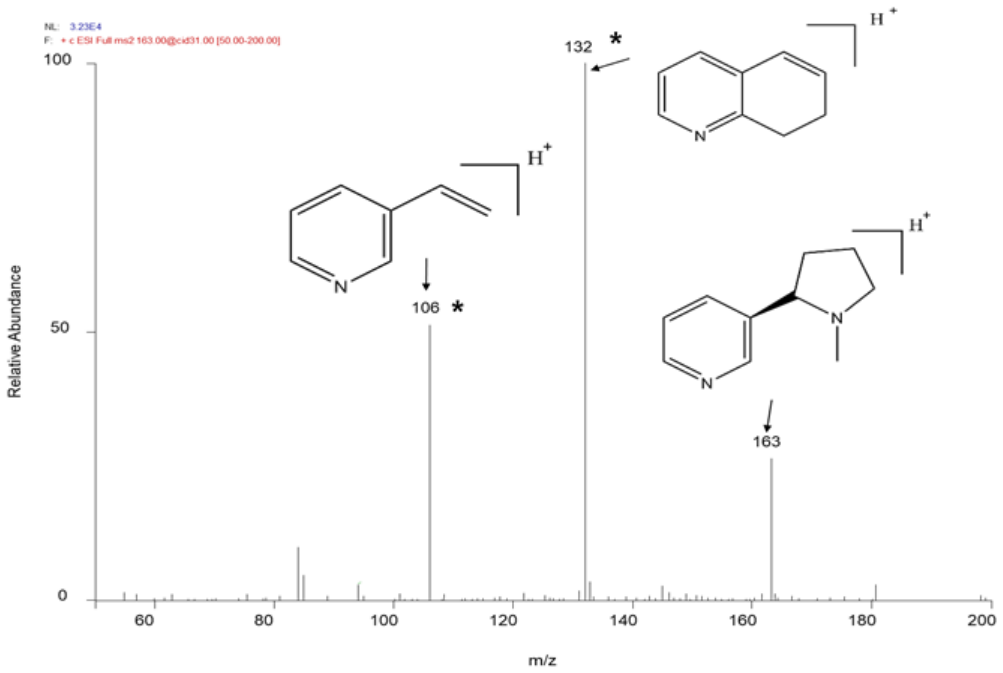

Figure 2.1 ESI MS/MS spectrum of nicotine.

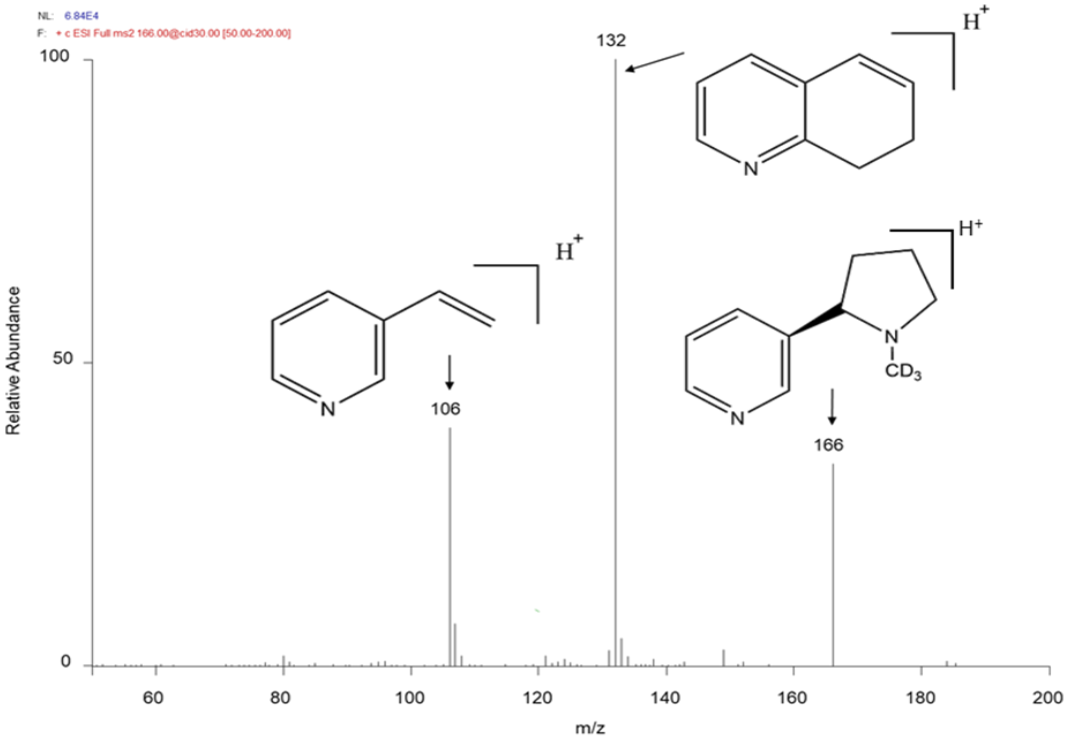

Figure 2.2 ESI MS/MS spectrum of nicotine-d_3.

Both nicotine and nicotine-d_3 eluted at 1.7 min. The MS/MS mode in full scan from range m/z 50-200 was used to distinguish the two different nicotine species. In this experiment, two channels are used to monitor the eluents. In one channel, an MS/MS experiment is performed monitoring the transition of m/z 163 Da → 132 Da. This channel is to follow nicotine. In the second channel, the transition is m/z 166 Da → 132 Da and is for the internal standard, nicotine-d_3. Tune methods were achieved from previous direct injection for this experiment. Figure 2.3 shows the results from a solution containing both types of nicotine. Isocratic elution was performed for the analysis using formic acid in water and acetonitrile as the mobile phases. Acetonitrile was selected for organic phase because it has higher elution strength leading to shorter analysis times and minimized background noise. Formic acid in mobile phase enhances ionization in positive mode for ESI of alkaloids. In addition, the reverse phase C_{18} column has lower backpressure to achieve good sensitivity. The addition of a buffer containing salts was avoided as mentioned in previous study,[9,14] in order to protect the ESI needle from clogging. The SIM mode was then used in the acquisition of data for the calibration curves and toenail samples.

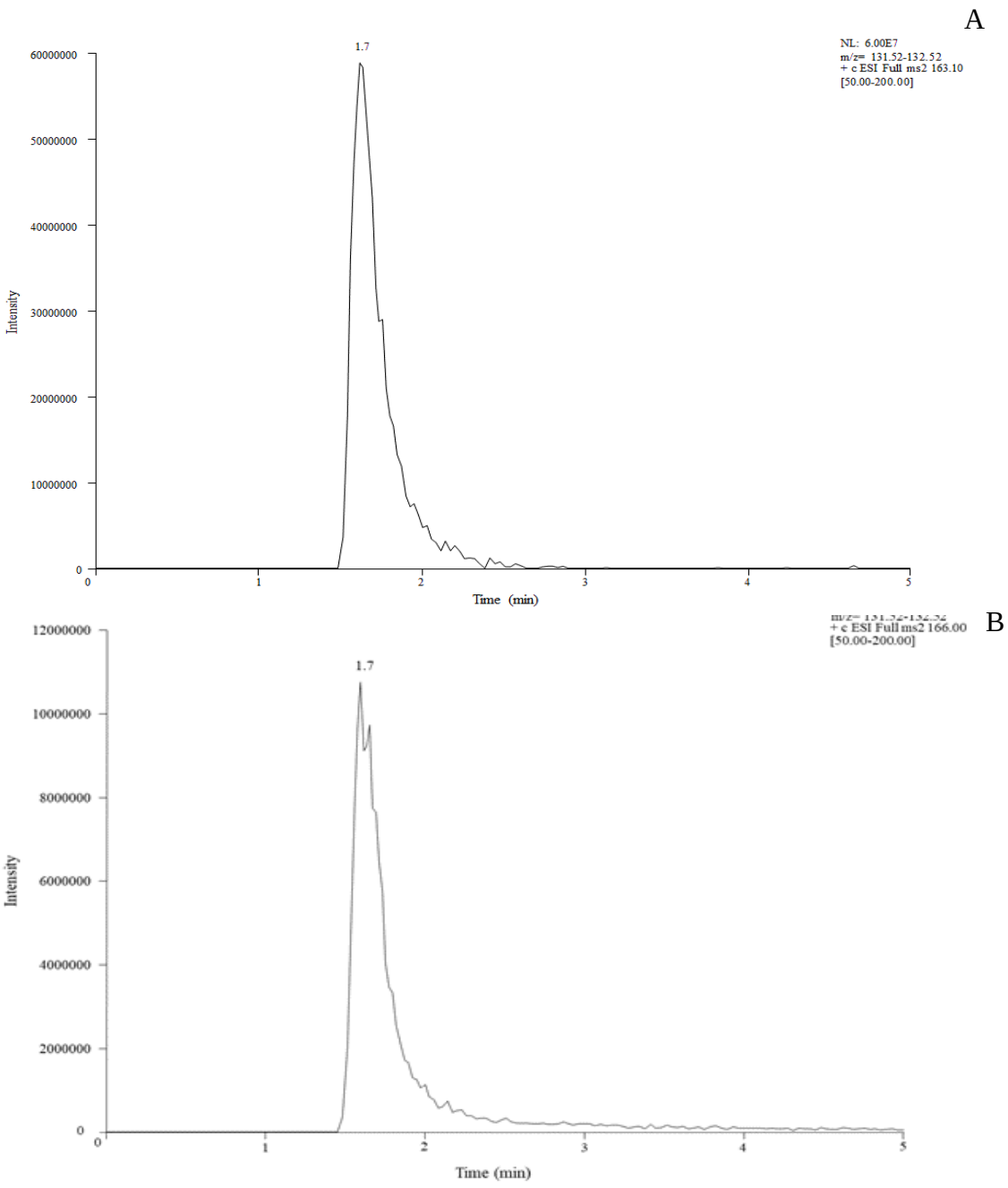

Figure 2.3 Representative MS/MS ion chromatograms. (A) nicotine ion (m/z 163 → 132 Da) and (B) nicotine-d3 ion (m/z 166 → 132 Da) during isocratic elution both showing a retention time of 1.7 minutes.

2.3.2 Solid phase extraction results

A part of the method development, we tried performing a solid phase extraction (SPE) using Sep-Pak Vac C18 Cartridges (Waters, MA) as a comparison to the liquid-liquid extraction. Two different SPE conditions were examined by using different eluent solvents. The first condition was proposed by Zuccaro et al,[15] included 7:3 ratio of isopropyl alcohol and dichloromethane, with 0.01% of HCl in methanol. The extract precipitated and did not dissolve in the HPLC solvent before analysis. Therefore, this first condition was not pursued further. The second condition used H_2O and methanol to treat the toenail sample and added the extracted sample to 0.01% of HCl in methanol. The second SPE condition achieved exhibited lower linearity comparing to liquid-liquid extraction for toenail sample analysis shown in Table 2.1.

Table 2.1 Comparison of the solid phase extraction methods for the detection of nicotine.

Method	**Eluent**	**Analyte**	**r^2**	**LOD, ng/mg**
SPE	Dichloromethane/isopropyl alcohol	Nicotine	N/A	N/A
SPE	Methanol	Nicotine	0.96	0.1

2.3.3 Method Validation

The developed method was validated for linearity, limit of quantitation, accuracy, precision, and recovery.[17] A toenail sample was spiked with nicotine and processed. A representative MS/MS ion chromatogram is showed as Figure 2.4 and exhibits the same retention time as that of the nicotine dissolved in the mobile phase. Calibration standards were prepared as mentioned in Section 2.2.2. The ratio of the nicotine peak area to that of the internal standard peak were used for creating a standard curve and calculating unknowns. The unspiked blank was subtracted from each standard before generating the regression line. Typically, a five calibration point curve was generated over the concentration range of 0.08 ng/mg to 20 ng/mg. A representative standard curve is shown as Figure 2.5. The standard curve is shown for using two different MS/MS ions (m/z 132 and 106 Da). These two ions are the major fragmentation ions from nicotine. Figure 2.5A shows the results using the 132 Da ion. Figure 2.5B are the results using the 106 Da ion.

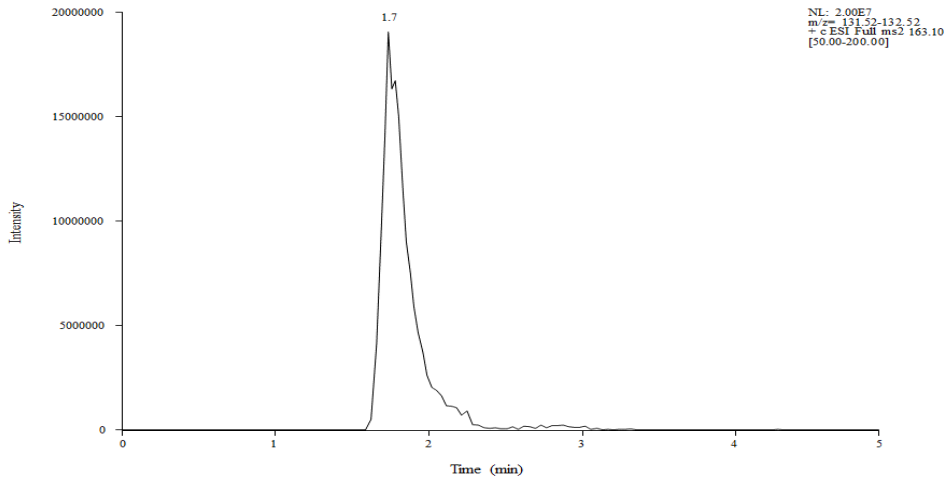

Figure 2.4 Representative MS/MS ion chromatogram of a nicotine spiked toenail sample.

The 132 Da ion is the most intense fragmentation ion and was selected for quantitative use. However, the lower mass ion also showed good linearity and can be used as a verification ion as needed.

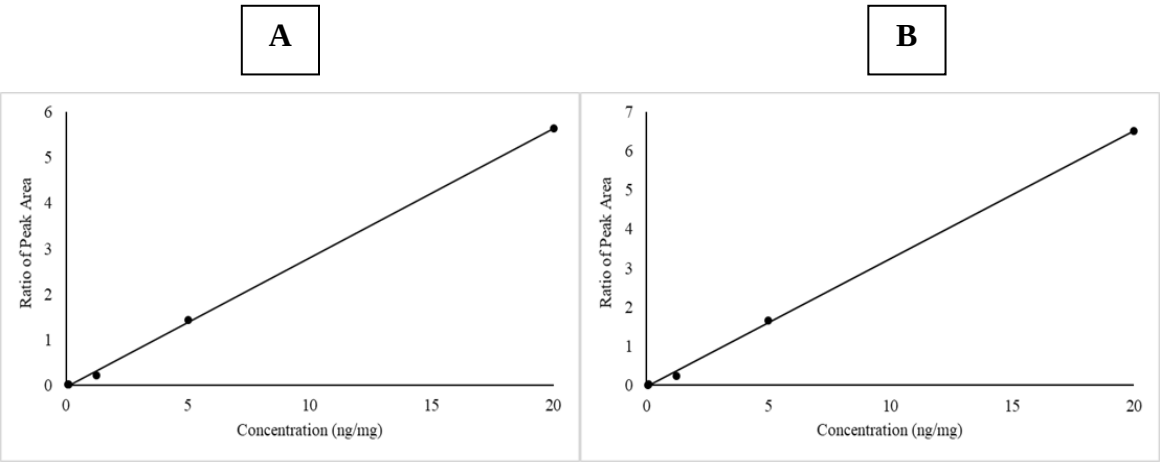

Figure 2.5 Nicotine calibration curves using the two major fragmentation ions at (A) m/z 132 and (B) m/z 106.

The figures of merit[17] for the developed method are summarized in Table 2.2 below. The limit of detection (LOD) is 0.005 ng/mg when using a 10 mg toenail sample. The limit of quantitation (LOQ), based on RSD < 20%, was determined to be 0.08 ng/mg for a 10 mg toenail sample. Both the LOD and the LOQ were experimentally determined by serial dilution until the signal to noise ratio was observed to be approximately 3 and 10, respectively. The precision (represented by the relative standard deviation, RSD) ranged from 0.8%-10.3% and meets the accepted range (RSD < 20%). The recovery[18] (RE) was determined at three different nicotine concentrations (0.08 ng/mg, 0.125 ng/mg, and 20 ng/mg), in triplicate, and were assessed by calculating the response of the extracted sample with analytes and the response of the post-extracted spiked sample using equation

2.1. Matrix Effect[18] (ME) were evaluated in the quantitative toenail analysis using equation 2.2. A positive ME stated that ion enhancement.

$$\% \text{ RE } = [\frac{\text{Response extracted sample with analytes}}{\text{Response post-extracted spike sample}}] \times 100 \quad (2.1)$$

$$\% \text{ ME} = ((\frac{\text{Response}_{\text{post-extracted spike sample}}}{\text{Response}_{\text{Solvent Standard}}})\text{-}1)\times 100 \quad (2.2)$$

Table 2.2. Figures of merit for the nicotine method.

Validation Parameters	**Toenail**
	Nicotine
Linearity Range (ng/mg)	0.08-20
r^2	0.998
LOD (ng/mg)	0.005
LOQ (ng/mg)	0.08
Precision (RSD%)	0.8%-10.3%
Recovery (%, n=3)	
Low Level	93.1%
Medium Level	88.7%
High Level	108.2%
Matrix Effect	Positive %, ion enhancement

2.4 Application

The developed method was tested using toenail samples that were collected from 7 individuals (author's friends and their age is over 18 years old). The MS/MS ion chromatogram (Figure 2.6) shows the results from an adult exposed to secondhand smoke. The retention time matches the standard solution chromatogram as depicted in Figure 2.3. For the secondhand smoke group, an individual had at least a 6 month exposure to a smoking environment, either from their roommates, partners or colleagues. The nicotine levels from the toenails are presented in Table 2.3; including a person exposed to secondhand smoke, a person not exposed to secondhand smoke, and active smokers. The mean nicotine level of individuals exposed to secondhand smoke and that of active smokers were 0.415 ng/mg and 1.75 ng/mg toenails, respectively. These results show that the levels of nicotine can be measured in toenails. Further, there is a large difference in the amount of nicotine between smokers and those exposed to secondhand smoke. Collection of data from a larger number of individuals will be needed to establish ranges of nicotine in the two groups. However, the initial results using this method are encouraging. It is also presumed that the information obtained from keratinic matrices provide a longer-term record of nicotine exposure. Although toenail nicotine levels were investigated previously by using HPLC-ECD, no other study has been reported assessing toenail nicotine levels using HPLC-MS. Our reported LOD of nicotine in toenails is 0.005 ng/mg and is lower than that previously reported for electrochemical detector analysis in toenails (LOD, 0.05 ng/mg).[19]

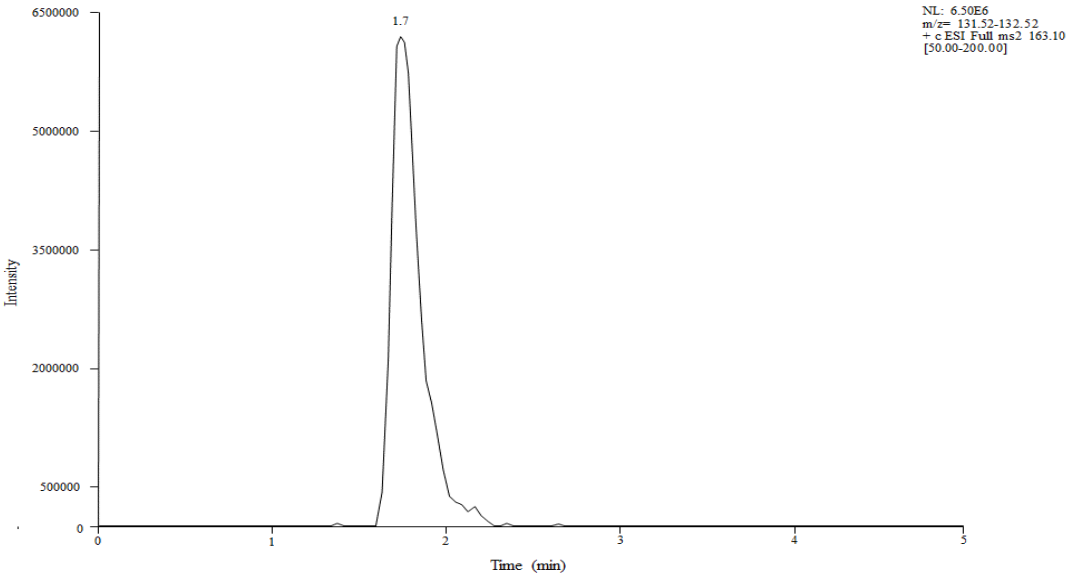

Figure 2.6 The nicotine MS/MS ion chromatogram for an adult exposed to secondhand smoke.

Table 2.3. Nicotine concentration in toenails from a person not exposed to secondhand smoke, a person exposed to secondhand smoke, and smoker.

Group	No. subjects	Mean Nicotine (ng/mg)	Exposed at Home	Exposed at Work
No exposure to secondhand smoke	3	0.103 ± 0.016	No	No
Exposed to secondhand smoke	2	0.415 ± 0.045	Yes	Occasionally
Smokers	2	1.75 ± 0.04	No	No

2.5 Conclusion

In conclusion**,** nicotine was successfully extracted by a liquid-liquid extraction method from toenails. The concentration of nicotine as measured in these samples using HPLC-MS. The methods developed here can be used for further tobacco alkaloid studies and in epidemiological biomarker studies.

2.6 References

1. *General Report of the Surgeon General. Reducing the health consequences of smoking: 25 years of progress;* DHHS publication CDC 89-8411; U.S. Department of Health and Human Services, Public Health Service, Centers for Disease Control, Center for Chronic Disease Prevention and Health Promotion, Office on Smoking and Health: Washington, DC, 1989.
2. R, Talhout.; T, Schulz.; E, Florek.; J, van Benthem.; P, Wester. *Int. J. Environ. Res. Public Health.* **2011**, *8*, 613-628.
3. *Respiratory Health Effects of Passive Smoking: Lung Cancer and Other Disorders;* NIH Publication 93-3605; U.S. Department of Health and Human Services, U.S. National Institutes of Health, U.S. National Cancer Institute: Washington, DC, 1993.
4. DeLeon, J.; Diaz, FJ.; Rogers, T.; et al. *J. Clin. Psychopharmacol.*, **2002**, 225, 496 – 501.
5. Jarvis, J.; Primatesta, P.; Erens, B.; et al. *Nicotine. Tob. Res.*, **2003**, *5*, 349 – 55.
6. Tosi, A.; Piraccini, B. Biology of Nails and Nail Disorders**.** In *Fitzpatrick's dermatology in general medicine***;** Freedberg, M.; Eisen, Z.; Wolff, K.; Ansten, F.; Goldsmith, A. Katz, I.; Fitzpatrick, B. Ed.; McGraw-Hill: New York, 1999.
7. Palmeri, A.; Pichini, S.; Pacifici, R.; et al. *Clin. Pharmacokinet.*, **2000**, *382*, 95-110.
8. Stepanov, I.; Feuer, R.; Jensen, J.; Hatsukami, D.; Hecht, S. S. *Cancer Epidemiol., Biomarkers Prev*., **2006**, *15*, 2378.
9. Mahoney, G.; Al-Delaimy, W. *J .Chromatogr. B Biomed. Appl*., **2001**, *753*, 179–187.

10. Bernert, J. T.; Alexander, J. R.; Sosnoff, C. S.; McGuffey, J. E. *J. Anal. Toxicol.*, **2011**, *35*, 1–7.
11. Miller, E. I.; Murray, G. J.; Rollins, D. E.; Tiffany, S. T.; Wilkins, D. G. *J. Anal. Toxicol*., **2011**, *35*, 321–332.
12. Pérez-Ortuño, R.; Martínez-Sánchez, J. M.; Fernández, E.; Pascual, J. A. *Anal. Bioanal. Chem.*, **2015**, *407*, 8463–8473.
13. Ho, CS.; Chan, MHM.; Cheung, RCK.; Law, LK.; Lit, LCW.; Ng, KF.; Suen, MWM.; Tai ,HL. *Clin. Biochem. Rev*., **2003**, *24*, 3–12.
14. Tuomi, T.; Johnsson, T.; Reijula, K. *Clin. Chem.*, **1999**, *45*, 2164–2172.
15. Zuccaro, P.; Altieri, I.; Rosa, M.; Passa, A.; Pichini, S.; Ricciarello, G.; Pacifici, R. *J. Chromatogr*. **1993**, *621*, 257–261.
16. Hariharan, M.; VanNoord, T. *Clin. Chem*. **1991**, *37*, 1276–1280.
17. Hopfgartner, G. *Anal. Bioanal. Chem.* **2020**, *412*, 531–532.
18. Matuszewski, B. K.; Constanzer, M. L.; Chavez-Eng, C. M. *Anal. Chem.*, **2003**, *75*, 3019– 3030.
19. Al-Delaimy, W. K.; Mahoney, G. N.; Speizer, F. E.; Willett, W. C. *Cancer Epidemiol., Biomarkers Prev*., **2002**, *11*, 1400.

Chapter 3: Standard Mimetic Lipoprotein Models

3.1 Introduction

In a study examining lethal diseases in North America, cardiovascular disease is the cause of 3% of all deaths.[1] According to the World Health Organization (WHO), there are approximately 17.7 million people who died of cardiovascular disease, representing one third of all global deaths in 2015.[2] High levels of lipoproteins associated with cholesterol have been a major risk factor in cardiovascular disease. Apolipoprotein B (ApoB-100), LDL (low density lipoprotein) and VLDL (very low density lipoprotein) play a critical role in proinflammatory and inflammatory mechanisms.[3] In addition, previous studies reported plasma cholesterol derived from LDL is predictive of coronary artery disease and that the plasma content levels of lipoproteins, such as triglycerides and cholesterol ester, may also contribute to cardiovascular disease.[4,5,6] In order to elucidate these major facts, medicine, biochemistry, and medical chemistry studies have primarily focused on developing new methods for prediction, prevention, and treatment of cardiovascular disease.

The structural characteristics of lipoprotein determine its amphipathicity and is based on the spherical shape of lipoprotein and its unique biomolecular function. Lipoproteins transport hydrophobic molecules in water, blood, and extracellular fluid. The outer shells of lipoproteins are made up of the hydrophilic head groups of phospholipids and esterified cholesterol, which are oriented towards to the aqueous environment. The internal core is comprised of cholesterol esters and triglycerides. Embedded apoproteins play a role in receptor proteins and determines the fate, in terms of receptor ligands, for a

majority of cells.[7] Apolipoproteins also direct the binding to membrane receptors and regulate enzymatic activity towards to the normal metabolism of lipoprotein.[8] The five classes of lipoproteins are defined by their size and density. They are chylomicrons, very low-density lipoprotein (VLDL), intermediate-density lipoprotein (IDL), low-density lipoprotein (LDL), and high-density lipoprotein (HDL). LDL is recognized as a "bad" lipoprotein. Cardiovascular disease and other relevant heart diseases are thought to be caused by higher LDL blood levels. LDL transports cholesterol into the body, accumulated cholesterol then coagulates on the arterial walls causing thickening and loss of elasticity. Conversely, HDL particles are referred as "good", because HDL functions as a "snowplow", breaking down and removing cholesterol deposited on the arterial walls.

There are a variety of studies examining mimetic lipoproteins. Thaxton and colleagues developed and elucidated lipoprotein mimetics for drug delivery.[9] Ohashi and Walker reported the use of lipoproteins to deliver chemotherapeutic and anticancer drugs.[10] Hayavi developed novel methods of biomimetic lipid supplement for serum free tissue culture.[11]

Although Brown and Goldstein were the first to define receptor-dependent atherosclerosis,[12] there are studies that have demonstrated and rendered the mimetic, or synthetic lipoprotein, as a model for research of cardiovascular disease or heart disease. Most clinical research has focused on using native lipoprotein, but the use of natural lipoprotein forms largely suppressed the experimental outcomes and analysis. This has been due in part to that it is not easy to collect human plasma infection and endotoxin free. This effect results in high cost and inconsistency to fulling research requirements

and only small quantities are obtained.[13,14] Moreover, there is the propensity for apoprotein contained in reconstituted LDL from native LDL to aggregate and not be stable.[15] The test for lipoprotein can also indirectly guide measurements that are more complex and redundant.[16,17] To avoid these issues, this study took the approach of replacing natural LDL with a mimetic lipoprotein model system and to ultimately support cardiovascular clinical analysis.[9,11,18]

This chapter is focused on the preparation of mimetic lipoproteins. The outcomes of these efforts will be discussed. UV-Vis and fluorescence spectroscopy were employed to evaluate the preparations. The Amplex Red cholesterol assay supported this study and help to verify that the mimetic lipoprotein preparation methods used in this study work as designed.

3.2 Material and Methods

3.2.1 Chemicals

DLPC (1,2-dilauroyl-sn-glycero-3-phosphocholine) and DOPG (1,2-dioleoyl-sn-glycero-3-phospho-(1'-rac-glycerol) were purchased from Avanti Polar Lipids, Inc (Alabaster, AL). The peptide, poly(LA)$_7$Y, was synthesized and purchased from Atlantic Peptides (Lewisburg, PA) with 95% purity. The complete 19 amino acid peptide sequence is as follows: KKLALYLALALYLALAKKW. All peptides were comprised of seven repeating leucine and alanine residues, and the amino terminus and carboxy terminus were both capped with lysine residues. The seven repeated leucine and alanine residues are likely embedded within the hydrophobic interior, which is sparingly soluble

in aqueous environments. Cholesterol, extra dry chloroform in molecular sieves, monosodium phosphate monohydrate, disodium phosphate heptahydrate, and sodium chloride were purchased from Fisher Scientific (Pittsburgh, PA). The Amplex Red Cholesterol Assay Kit was purchased from Thermo Fisher Scientific (Waltham, MA).

3.2.2 Peptide Preparation

1 mg of synthetic peptide was dissolved in 1.2 ml of 1,1,1,3,3,3-hexafluoro-2-propanol (HFIP) (Sigma Aldrich, St. Louis, MO), and distributed among test tubes so that each tube held 0.05 mg of peptide. The HFIP was then removed under a stream of argon gas while rotating the test tube to evenly dry the peptide.

3.2.3 Synthetic Standard Lipoprotein Preparation

25 mg/ml of DOPG, DLPC, and cholesterol were prepared in chloroform and combined to form 0 and 15 percent cholesterol, 30 percent DOPG by weight, with the remaining weight comprised of DLPC in glass culture tubes. Simultaneously, 25 mg/mL of DOPG, DLPC, and cholesterol were prepared in chloroform and combined to form 0, 15, 30 percent cholesterol, 30 percent DOPG by weight, with the remaining weight comprised of DLPC in glass culture tubes. The chloroform was then evaporated under a stream of argon to leave an oil-like film on the bottom of the tube. The tube was then dried overnight in a vacuum desiccator. The dried samples were then rehydrated by adding 20 mM phosphate buffer (pH 7.4) with sonication in a bath sonicator for 3 hours at 50°C until the solutions changed from cloudy to opaque. The resulting solutions were diluted to 5 mg/mL and then combined with dried peptide for a final concentration of 90

μM. The resulting solutions were stored at room temperature to ensure peptide insertion and equilibrium. The liposome containing peptide and 0, 15 %, and 30% cholesterol were centrifuged using a Sorvall WX 80+ Ultracentrifuge (Thermo, USA) at 213,373 × g and 4°C for 2 h. The supernatant was discarded and the sample was reconstituted with 1 mL of 20 mM phosphate buffer. The size of liposome formed from this preparation was confirmed at 20°C by DLS (dynamic light scattering, Dyna Pro, Wyatt Technology Corp., Santa Barbara, CA) measurements. The mean hydrodynamic radius was typically in the range of 40 ± 0.39 nm, regardless of the covesicallized particle (DPH).

3.2.4 Spectroscopy Measurements

The peptide concentration in the mimetic lipoprotein model was monitored by UV-Vis absorption using a Varian Cary 50 UV-Vis spectrophotometer (Palo Alto, CA). The wavelengths were scanned from 200 nm to 800 nm. Peptide insertion was verified by fluorescence using a Varian Cary Eclipse spectrophotometer (Palo Alto, CA). All prepared samples were excited at 280 nm, and emission was detected from 300 nm to 400 nm.

3.2.5 Fluorescence Anisotropy Measurement

DPH was used to determine the fluorescence anisotropy of the liposomes. All fluorescence anisotropy measurements were performed on a Cary Eclipse fluorometer. A manual polarizer and the following experimental conditions were employed:[19] λ_{ex} = 360

nm, λ_{em} = 430 nm, [DPH] = 0.5 µM, and [lipids+cholesterol] = 50 µM. Equation 3.1 was used to determine the fluorescence anisotropy,[20] r,

$$r = \frac{I_{VV} - GI_{VH}}{I_{VV} + 2GI_{VH}}, G = \frac{I_{HV}}{I_{HH}} \quad (3.1)$$

where IVV is the fluorescence intensity with excitation and emission polarized in the vertical position, IVH is the fluorescence intensity with excitation in the vertical position and the emission in the horizontal position, IHV and IHH stands for both fluorescence intensity with excitation in the horizontal position, and emission in the horizontal and vertical position, respectively. The grating factor G is an instrumental correction factor for the emission optics for the vertical orientation to horizontal orientation. The fluorescence anisotropy of the lipoproteins was observed the temperature the range of 0 - 40°C. The temperature controller in the fluorometer was regulated by Neslab RTE-111 temperature control unit.

3.2.6 Amplex Red Cholesterol Assay Kit

Only the 15% by weight cholesterol in liposomes solutions were analyzed using the Amplex Red Cholesterol assay. The samples were dissolved in the given buffer from the cholesterol assay kit and diluted to 30 µg/mL. 50 µL of each diluted sample was pipetted into separate wells of a microplate. Other instructions for the preparation of standard and enzymatic reaction probes followed the instructions with the Amplex Red Cholesterol assay kit. All samples, reference standards, and background samples were incubated in

the microplate using a Biotek SynergyMX fluorescence microplate reader (Winooski, VT).

3.2.7 Data Analysis

All data were processed in the MATLAB environment, version 9.4 (MathWorks, Natick, MA).

3.3 Results and Discussion

3.3.1 Measurement of Cholesterol Concentration Using the Amplex Red Cholesterol Assay

A standard cholesterol calibration curve (Figure 3.1) was generated using the Amplex Red cholesterol assay, which is a simple fluorometric method for quantifying cholesterol. The Amplex Red cholesterol assay is used to measure the total cholesterol content in a sample via an enzymatic reaction. The use of fluorescence results in a highly sensitive indirect assay for cholesterol. The calibration standard curve (R^2>0.99) was used to determine the amount of cholesterol present in liposomes.

A technique of extrusion is utilized homogenizing lipids to give clearer spectroscopic characterization of the lipids.[21,22] Although there are previous studies of liposomes with cholesterol using extrusion, [23] extrusion was avoided in this study because of the large loss of cholesterol during the extrusion process.

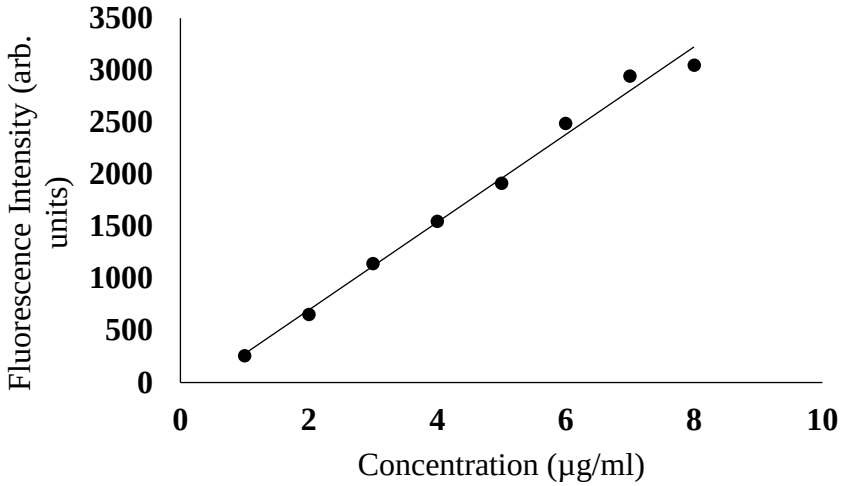

Figure 3.1 Cholesterol reference standard curve. Cholesterol standard solutions are mixed into the reaction buffer (0.1 M potassium phosphate, pH7.4, 0.5 M NaCl, 5 mM cholic acid, 0.1% triton X-100) to produce cholesterol concentrations of 0 to 8 µg/mL.

The estimated cholesterol content in the liposomes was greatly reduced after extrusion as indicated in Table 3.1. There is a reduced cholesterol content due to the high viscosity of cholesterol in the prepared lipids and these were unable to pass through the membrane filter during extrusion.

Table 3.1 Amplex Red assay results for liposomes with 15% cholesterol by weight. At intensity 11674 counts (sonication only) and at intensity 6292 counts (sonication and extrusion).

Methods	**Intensity**	**Concentration (µg/ml)**
No Extrusion	11674	28.07
Extrusion	6292	15.27

3.3.2 Spectroscopic identification and characterization of mimicking lipoprotein model

The fluorescence anisotropy of 1,6-diphenyl-1,3,5-hexatriene (DPH) was used to determine the fluidity of liposomes with varying amounts of cholesterol. DPH is a fluorescent hydrocarbon used to study cell membranes, it showed a strong fluorescence intensity in lipids. DPH serves as dye for cholesterol in the mimicking liposome model. The fluorescence spectrum of DPH is shown as Figure 3.2.

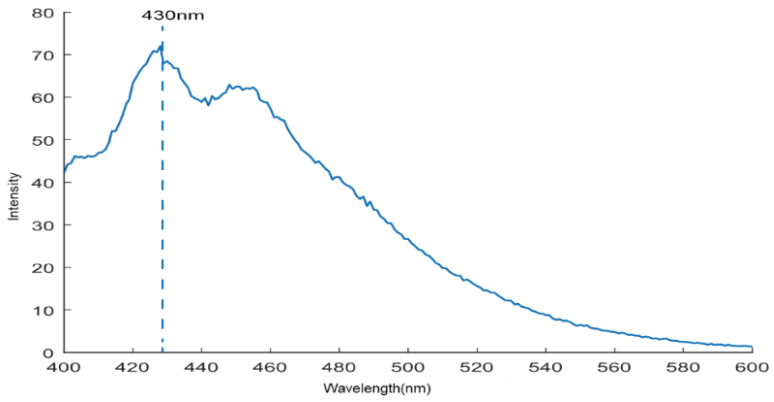

Figure 3.2 Fluorescence emission spectrum of DPH (1,6-diphenyl-1,3,5-hexatriene).

The cholesterol content can determine the membrane fluidity associated with cardiovascular disease in lipoprotein research.[24,25,26] This study first investigates the membrane fluidity correlation with cholesterol. The fluorescence anisotropy, r (equation 3.1) vs temperature is displayed in Figure 3.3. In Figure 3.3, as the temperature is increased, the anisotropy decreased. This indicates that membrane fluidity increased with associating amounts of cholesterol from 0 to 30%. A previous study using a sterol, a

cholesterol analog, demonstrated that increasing amounts of the sterol decreased membrane fluidity over the temperature range of 7 to 37°C.[27]

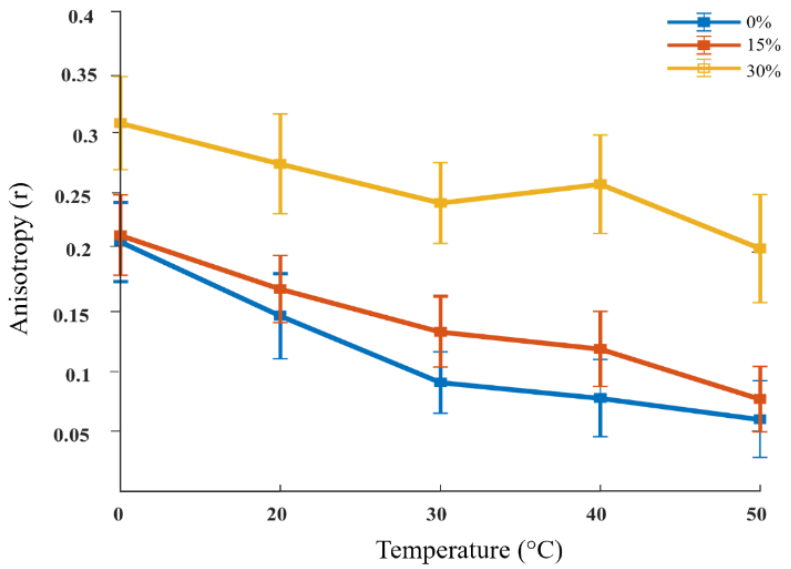

Figure 3.3 Fluorescence anisotropy of DPH in liposomes containing 0% cholesterol (blue), 15% cholesterol (red), and 30% cholesterol (yellow) by weight. Error bars indicate the standard deviation of the fluorescence anisotropy for three replicate sample preparations.

This study used UV-Vis spectrophotometry to identify the peptide poly $(LA)_7$ and fluorescence to verify peptide insertion. UV-Vis absorbance spectra with an absorbance peak at 280 nm can be used to indicate the presence of a tryptophan residue. Figure 3.4 shows the UV-Vis spectra for DLPG, poly$(LA)_7$Y in liposome without cholesterol, and 15% cholesterol by weight with poly$(LA)_7$Y in the liposome. The presence of the peak at 280 nm identifies the peptide in liposome.

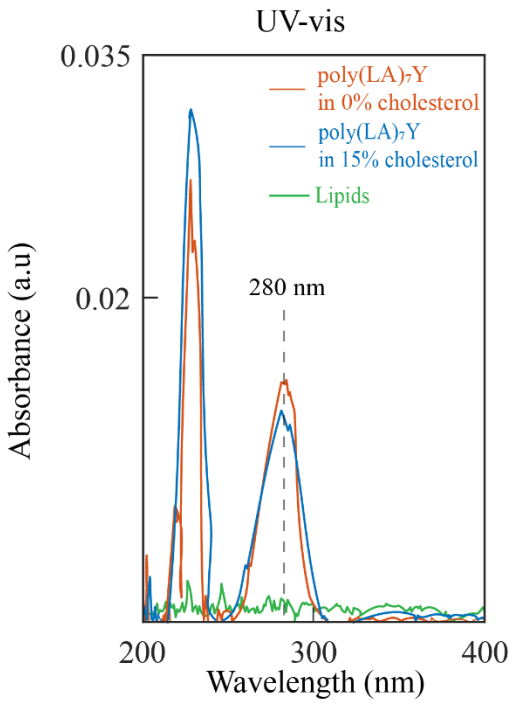

Figure 3.4 Absorption spectrum of tryptophan in poly(LA)$_7$Y. Tryptophan absorbed UV light at 280 nm (red) and with 15% cholesterol weight in DLPG (blue).

Poly(LA)$_7$ insertion into the liposome can to serve as an apolipoprotein to mimic the lipoprotein environment. To further verify if this peptide has inserted into the liposome, fluorescence measurements were performed. Natural lipoprotein features amphipathicity, and tryptophan fluorescence modes are environmentally sensitive. This can be used to monitor hydrophobic environments.[28,29] In fluorescence, peptide Poly(LA)$_7$Y with a tryptophan residue on the c-terminus in aqueous solution indicated a maximum emission wavelength at 362 nm in Figure 2.5A. A slight blue shift was observed in Figure 2.5 B and this tryptophan feature is due to peptide insertion for both the peptide containing the liposome and with 15% cholesterol by weight with peptide in the liposome.

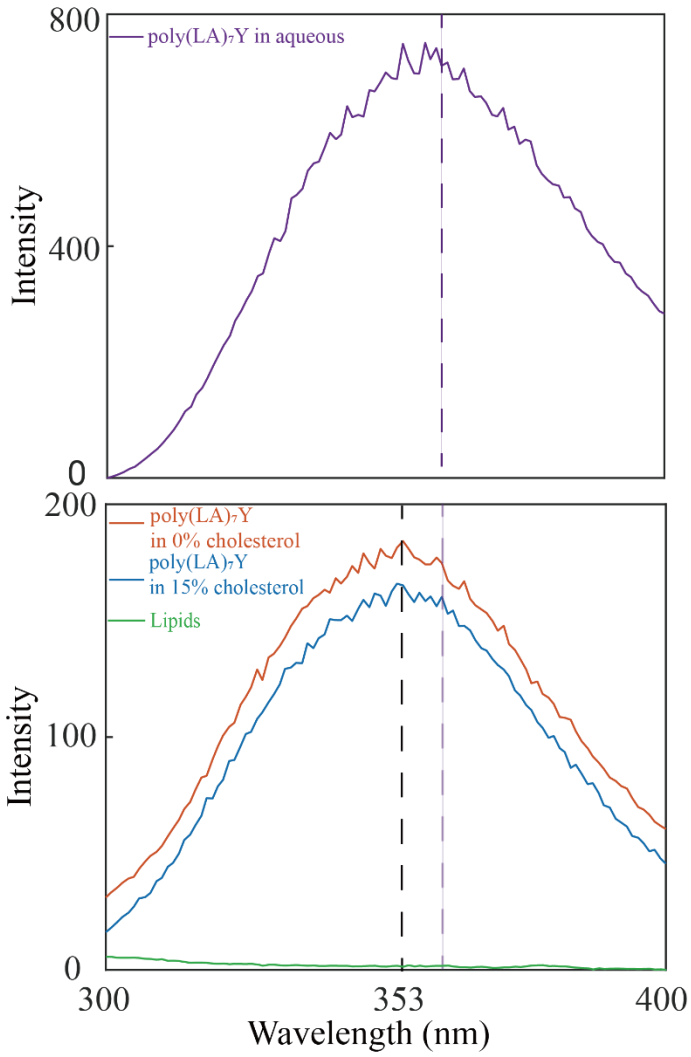

Figure 3.5 (A) Fluorescence of tryptophan in poly(LA)$_7$Y. λ_{ex}=280 nm, λ_{em}=362 nm in aqueous environment. (B) Fluorescence of tryptophan in poly(LA)$_7$Y. λ_{ex}=280 nm, λ_{em}=353 nm in liposome (red), tryptophan in poly(LA)$_7$Y with 15% cholesterol by weight in DLPG (blue), and liposome only (green).

3.3 Conclusion

This study focused on method development of mimicking lipoproteins and demonstrated an overview lab made mimetic lipoprotein models. Mimetic lipoprotein models were identified by types of spectrophotometers and each process was also well

explained. Another independent study of measuring cholesterol was also performed to verify its purpose as well.

3.4 References

1. Nordestgaard, B. G.; Chapman, M. J.; Ray, K.; Borén, J.; Andreotti, F.; Watts, G. F.; Ginsberg, H.; Amarenco, P.; Catapano, A.; Descamps, O. S.; Fisher, E.; Kovanen, P. T.; Kuivenhoven, J. A.; Lesnik, P.; Masana, L.; Reiner, Z.; Taskinen, M.-R.; Tokgözoglu, L.; Tybjærg-Hansen, A., *European Heart Journal* **2010,** 31, 2844-2853.
2. Benjamin, E. J.; Blaha, M. J.; Chiuve, S. E.; Cushman, M.; Das, S. R.; Deo, R.; de Ferranti, S. D.; Floyd, J.; Fornage, M.; Gillespie, C.; Isasi, C. R.; Jiménez, M. C.; Jordan, L. C.; Judd, S. E.; Lackland, D.; Lichtman, J. H.; Lisabeth, L.; Liu, S.; Longenecker, C. T.; Mackey, R. H.; Matsushita, K.; Mozaffarian, D.; Mussolino, M. E.; Nasir, K.; Neumar, R. W.; Palaniappan, L.; Pandey, D. K.; Thiagarajan, R. R.; Reeves, M. J.; Ritchey, M.; Rodriguez, C. J.; Roth, G. A.; Rosamond, W. D.; Sasson, C.; Towfighi, A.; Tsao, C. W.; Turner, M. B.; Virani, S. S.; Voeks, J. H.; Willey, J. Z.; Wilkins, J. T.; Wu, J. H.; Alger, H. M.; Wong, S. S.; Muntner, P., *Circulation* **2017.**
3. Packard, C. J.; Demant, T.; Stewart, J. P.; Bedford, D.; Caslake, M. J.; Schwertfeger, G.; Bedynek, A.; Shepherd, J.; Seidel, D., *J. Lipid Research* **2000**, 41, 305-317.
4. Ross, R., *Am. Heart J **1999,*** 138, S419-S420.
5. Motta, M.; Bennati, E.; Cardillo, E.; Ferlito, L.; Passamonte, M.; Malaguarnera, M., *Archives of Gerontology and Geriatrics* **2009,** 49, 162-164.
6. Malaguarnera, M.; Vacante, M.; Avitabile, T.; Malaguarnera, M.; Cammalleri, L.; Motta, M., *The Am. J. Clin. Nutrition* **2009**, 89, 71-76.

7. Hevonoja, T.; Pentikäinen, M. O.; Hyvönen, M. T.; Kovanen, P. T.; Ala-Korpela, M., *Biochim. Biophys. Acta (BBA) - Molecular and Cell Biology of Lipids* **2000,** 1488, 189-210.
8. Feingold, K. R.; Grunfeld, C. *Introduction to Lipids and Lipoproteins.* MDText.com, Inc., South Dartmouth (MA): **2000.**
9. Thaxton, C. S.; Rink, J. S.; Naha, P. C.; Cormode, D. P., *Advanced Drug Delivery Reviews* **2016**, 106, Part A, 116-131.
10. Gal, D.; Ohashi, M.; MacDonald, P. C.; Buchsbaum, H. J.; Simpson, E. R., *Am. J. Obstet. Gynecol* **1981***,* 139, 877-885.
11. Hayavi, S.; Halbert, G. W., *Biotechnol. Prog* **2005**, 21, 1262-1268.
12. Brown, M.; Goldstein, J., *Science* **1986,** 232, 34-47.
13. Patsch, J. R.; Sailer, S.; Kostner, G.; Sandhofer, F.; Holasek, A.; Braunsteiner, H., *J. Lipid Res* **1974**, 15, 356-366.
14. Sviridov, D.; Remaley, A. *Biochem J* . **2015**, 472 (3), 249–259.
15. Shrivastava, M.; Jain, A.; Gulbake, A.; Hurkat, P.; Jain, N.; Vijayraghwan, R.; Jain, S. K., *Scientia Pharmaceutica* **2014**, 82, 873-888.
16. Cooper, G. R.; Smith, S. J.; Duncan, I. W.; Mather, A.; Fellows, W. D.; Foley, T.; Frantz, I. D.; Gill, J. B.; Grooms, T. A.; Hynie, I., *Clin. Chem* **1986**, 32, 921-929.
17. Abell, L. L.; Levy, B. B.; Brodie, B. B.; Kendall, F. E., *J. Biol. Chem.* **1952**, 195, 357-366.
18. Baillie, G.; Owens, M. D.; Halbert, G. W., *J. Lipid Res* **2002**, 43, 69-73.
19. Hebrant, M.; Tecilla, P.; Scrimin, P.; Tondre, C., *Langmuir* **1997**, 13, 5539-5543.

20. *Fluorescence Anisotropy: In Principles of Fluorescence Spectroscopy.* Lakowicz, J. R., Ed. Springer US: Boston, MA **2006**; pp 353-382.
21. Akbarzadeh, A.; Rezaei-Sadabady, R.; Davaran, S.; Joo, S. W.; Zarghami, N.; Hanifehpour, Y.; Samiei, M.; Kouhi, M.; Nejati-Koshki, K. *Nanoscale Res. Lett*. **2013**, *8* (1), 102.
22. Frisken, B. J.; Asman, C.; Patty, P. J. *Langmuir* **2000**, *16* (3), 928–933.
23. Nikanjam, M.; Blakely, E. A.; Bjornstad, K. A.; Shu, X.; Budinger, T. F.; Forte, T. M., *Int. J. Pharm* **2007**, 328, 86-94.
24. Pritchard, K. A.; Schwarz, S. M.; Medow, M. S.; Stemerman, M. B. Am. J. Physiol.: Cell Physiol. **1991**, *260* (1), C43–C49.
25. Yang, S.-T.; Kreutzberger, A. J. B.; Lee, J.; Kiessling, V.; Tamm, L. K. *Chem Phys Lipids*. **2016**, *199*, 136–143.
26. Pritchard, K. A.; Groszek, L.; Smalley, D. M.; Sessa, W. C.; Wu, M.; Villalon, P.; Wolin, M. S.; Stemerman, M. B. *Circ. Res.* **1995**, *77* (3), 510–518.
27. Eagleburger, M. K.; Cooley, J. W.; JiJi, R. D., *Biopolymers* **2014**, 101, 895-902.
28. Vivian, J. T.; Callis, P. R. *Biophys. J.* 2001, 80, 2093–2109.
29. Ladokhin, A. S.; Jayasinghe, S.; White, S. H. *Anal. Biochem.* **2000**, *285* (2), 235–245.

Chapter 4: Analysis of a mimetic lipoprotein model by Deep UV-Vis Resonance Raman Spectroscopy

4.1 Introduction

Heart disease is leading causes of death in the United States and rates are surprisingly high, accounting for about 1 in 4 deaths each year.[1] Some key factors that indicate health risk of heart disease are high blood pressure, high blood cholesterol, and smoking. Cholesterol levels are often measured as a diagnostic for heart disease. Cholesterol is either hydrophobic or blood insoluble. It attaches to a protein called lipoprotein that transports cholesterol throughout body. Lipoproteins have a spherical-like shape coiled with apolipoprotein and the entire outer shell is surrounded by phospholipids and free cholesterol. The core is composed of hydrophobic triglycerides and cholesteryl esters. Lipoproteins are classified by five major class according to particle size and density. They are chylomicrons, very low-density lipoprotein (VLDL), intermediate density lipoprotein (IDL), low density lipoprotein (LDL), and high density lipoprotein (HDL). Chylomicrons are rich in triglycerides and low in proteins. Inversely, high density lipoprotein has largest protein content. Total cholesterol measurements are common clinical tests to assess and predict heart disease. An elevated concentration of low-density lipoprotein cholesterol is a higher risk of heart disease, whereas increases in high density lipoprotein will decrease the risk of heart disease. However, clinical tests still have hurdles when measuring low density and high-density lipoproteins directly because cholesterol, lipoprotein size, and density vary from person to person.[2,3] The treatments for heart disease resulting from these measurements are varied and can lead to inefficient and inaccurate treatments. A direct estimation of LDL level has been

calculated by using the Friedewald equation, but it is limited specific conditions and considerable discrepancies of estimation.[4,5] Alternatively, LDL levels were isolated and measured using immunochemical adsorption. These methods were imprecise and high measurement error rates.[6] High density lipoprotein is mostly measured using refined techniques in clinical settings, such as ultracentrifugation, electrophoresis, high performance liquid chromatography (HPLC), and NMR. In these methods, the cholesterol content was measured by precipitation of apoprotein in the lipoproteins. In ultracentrifugation, various types of apolipoproteins are poorly separated. This result leads to uncertainties in the level of apoproteins and make this important biomarker difficult to use in predicting health risks.[7] There are two types of electrophoresis methods used to measure high density lipoproteins, they are gradient gel ND-PAGGE and 2D-PAGGE respectively.[8,9] However, there is little data about these techniques and measurements to predict HDL level and associating them with heart disease. In addition, HPLC and NMR require additional specifications when measuring HDL.[10,11,12] Deep UV-Vis Resonance Raman (dUVRR) spectroscopy has been emerged in the analysis of plasma lipoproteins. Components (cholesterol, triglycerides, apoproteins and phospholipids) contained in lipoproteins are commonly and independently analyzed by dUVRR spectroscopy due to its advantages of enhancing signal of individual components in complex samples. Moreover, free labeling and non-destructive measurements provided more accurate results in temperature and chemically sensitive components, such as apoproteins.[13,14,15] However, measuring large quantities of lipoproteins requires significant sample preparation and pretreatments before dUVRR spectroscopy measurements. Further, the high cost of commercially prepared lipoproteins makes their

availability to researchers difficult. A limited number of studies have obtained information about cardiovascular clinical research and correlated the results with each class of lipoproteins. Biomimetic lipoprotein models provide non-toxic, non-immunogenic, and biocompatible sample that can be used in a number of laboratory-based studies. Biomimetic lipoproteins can be used to generate different types of lipoproteins including particle size, cholesterol content, and apoproteins for further clinical research needs.[16] In addition, biomimetic models allow for longer storage times for research purposes. dUVRR protein/peptide spectra have four distinguished amide modes. The amide I band consists of features contributing to the carbonyl stretch (C=O) vibration. The region of the amide I band often occurs between 1600 to 1690 cm^{-1}.[17] Amide II region designates the out-of-phase combination of the C-N stretch and N-H in-plane bending. They mostly occur in region of 1450-1580 cm^{-1}. The N-H in-plane bending constitutes about 60% of the intensity in this region.[18] The amide III band is the in-phase combination of C-N stretching, N-H in plane bending, and C_α-C stretching. This region is usually observed between 1200 and 1300 cm^{-1}. The amide S band (S means sensitivity to secondary structure) is a combination C_α-H bend/N-H bend coupled with Amide III. However, the Amide S band is more likely due to β-sheets and is not resonantly enhanced in α-helical conformations. This band is observed at 1315-1425 cm^{-1}. [19, 20, 30] In this study, we combine dUVRR spectroscopy, a non-invasive technique with smaller sample amounts to generate spectra we can use to characterize lipoprotein models.

4.2 Material and Methods

4.2.1 Chemicals

DLPC (1,2-dilauroyl-sn-glycero-3-phosphocholine) and DOPG (1,2-dioleoyl-sn-glycero-3-phospho-(1'-rac-glycerol) were purchased from Avanti Polar Lipids, Inc (Alabaster, AL). The peptide, poly(LA)$_7$Y, was synthesized and purchased from Atlantic Peptides (Lewisburg, PA) with 95% purity. 20 mM phosphate buffer with 5 mM saline at pH=7.4 was prepared by 18.2 MΩ-cm water (Barnstead). $NaClO_4$ (0.1 mM sodium perchlorate, Sigma Aldrich, ≥ 98%) were prepare as an internal standard solution for dUVRR spectroscopy measurements. The complete 19 amino acid peptide sequence is as follows: KKLALYLALALYLALAKKW. All peptides were comprised of seven repeating leucine and alanine residues, and the amino terminus and carboxy terminus were both capped with lysine residues. The seven repeating leucine and alanine residues are likely embedded within the hydrophobic interior, which is sparingly soluble in aqueous environments. Cholesterol, extra dry chloroform in molecular sieves, monosodium phosphate monohydrate, disodium phosphate heptahydrate, and sodium chloride were purchased from Fisher Scientific (Pittsburgh, PA). The Amplex Red Cholesterol Assay Kit was purchased from Thermo Fisher Scientific (Waltham, MA).

4.2.2 Peptide Preparation

1 mg of synthetic peptide was dissolved in 1.2 mL of 1,1,1,3,3,3-hexafluoro-2-propanol (HFIP) (Sigma Aldrich, St. Louis, MO), and distributed among test tubes so that each tube held 0.05 mg of peptide. The HFIP was then removed under a stream of argon gas while rotating the test tube to evenly dry the peptide.

4.2.3 Synthetic Standard Lipoprotein Preparation

25 mg/mL of DOPG, DLPC, and cholesterol were prepared in chloroform and combined to form 0 and 15 % cholesterol into DOPG by weight, with the remaining weight comprised of DLPC in glass culture tubes. The chloroform was then evaporated under a stream of argon to leave an oil-like film on the bottom of the tube. The tube was then dried overnight in a vacuum desiccator. The dried samples were then rehydrated by adding 20 mM phosphate buffer (pH 7.4) with sonication in a bath sonicator for 3 hours at 50°C until the solutions changed from cloudy to opaque. The resulting solutions were diluted to 5 mg/mL and then combined with dried peptide for a final concentration of 90 µM. The resulting solutions were stored at room temperature to ensure peptide insertion and equilibrium. The size of liposome formed from this preparation was confirmed at 20°C by DLS (dynamic light scattering, Dyna Pro, Wyatt Technology Corp., Santa Barbara, CA) measurements. The mean hydrodynamic radius was in the range of 40 ± 0.39 nm, regardless of the covesicallized particle (DPH). The liposome containing peptide and 0, 15 %, and 30% cholesterol were centrifuged using a Sorvall WX 80+ Ultracentrifuge (Thermo, USA) at 213,373 × g and 4°C for 2 h. The supernatant was discarded and the sample was reconstituted with 1 mL of 20 mM phosphate buffer. 50 µL of 0.1 mM $NaClO_4$ was added in both 0 and 10 % as an internal standard for dUVRR analysis.

4.2.4 Spectroscopy Measurements

The peptide concentration in the mimetic lipoprotein model was monitored by UV-Vis absorption using a Varian Cary 50 UV-Vis spectrophotometer (Palo Alto, CA). The wavelengths were scanned from 200 nm to 800nm. Peptide insertion was verified by fluorescence using a Varian Cary Eclipse spectrophotometer (Palo Alto, CA). All prepared samples were excited at 280 nm, and emission was detected from 300 nm to 400 nm.

CD measurements were collected on a Jasco J-710 CD spectropolarimeter (Easton, MD) with a 1-mm path length cuvette (Hellma, Plainview, NY). Samples were scanned from 190 nm to 250 nm with scan speed of 50 nm/min and a response time of 4 s. Each spectrum was the average of five replicate scans. All spectra were blank subtracted and converted to mean residue ellipticity θ ($deg \cdot cm^2 \cdot dmol^{-1}$).

Raman spectroscopy was used to characterize the mimetic lipoprotein models. Collecting Raman spectra made use of the soft laser generated by Indigo-S laser system (Coherent Inc., Santa Clara, CA). The system used the fourth harmonic of a 4 kHz frequency quadrupled Ti:Sapphire laser. The Ti:Sapphire laser was pumped using a diode-pump frequency doubled Nd:YLF laser (Coherent Inc., Santa Clara, CA). The samples were excited at 197 nm and the average power of incident laser at the sample approximately 0.5 mW to minimize potential degradation. All samples were held in a custom-made water-jacked reservoir (Mid River Glassblowing, St Charles, MO) and the sample was introduced using a circulating system, model 7511-10 gear pump (Cole Palmer, Vernon Hills, IL). An Isotemp 3016D circulating water bath (Fisher Scientific,

Pittsburgh, PA) was use to maintain the sample temperature at 7°C. A nitrogen gas stream was flowed over the samples to ensure removal of ambient oxygen. The detector contained a back illuminated, phosphor coated, liquid nitrogen cooled Symphony CCD camera (Horiba Jobin Yvon Inc., Edison, NJ) with 2048 × 512 pixels. A final resolution of 2.4 cm^{-1} was in used in the collection of data. In addition, the spectrometer design had a 135° backscattering geometry and a 1.25 m spectrophotometer fitted with 3600 groove/mm grating to disperse and collect Raman scattering. Spectra were calibrated using a standard cyclohexane spectrum. Samples were signal averaged using five 60 s scans and were measured in triplicate.

4.2.5 Data Analysis

All data were processed and analyzed using Matlab 9.4 (Mathworks, Natick, MA).

4.3 Results and Discussion

4.3.1 Peptide Verification and Insertion in UV-Vis and Fluorescence

The peptide, poly $(LA)_7$, was selected to serve as a putative apoprotein in lipoproteins in this study. UV-Vis spectrophotometry was applied to identify the peptide and fluorescence was used to verify peptide insertion. UV-Vis absorbance spectra with an absorbance peak at 280 nm can be used to indicate the presence of a tryptophan residue. Figure 4.1 shows the UV-Vis spectra of DLPG, poly$(LA)_7$Y in liposome without cholesterol, and 15% cholesterol by weight with poly$(LA)_7$Y in the liposome. The presence of the peak at 280 nm identifies the peptide in liposome. In addition, the

absorption *A* was plotted in the following equation to calculate peptide concentration for CD data interpretation.

$$c = \frac{A}{l\varepsilon_{trp}} \tag{4.1}$$

where A is absorbance at 280 nm, *l* is pathlength in cm, and ε_{trp} is extinction coefficient representing tryptophan at 5500 $M^{-1}cm^{-1}$.

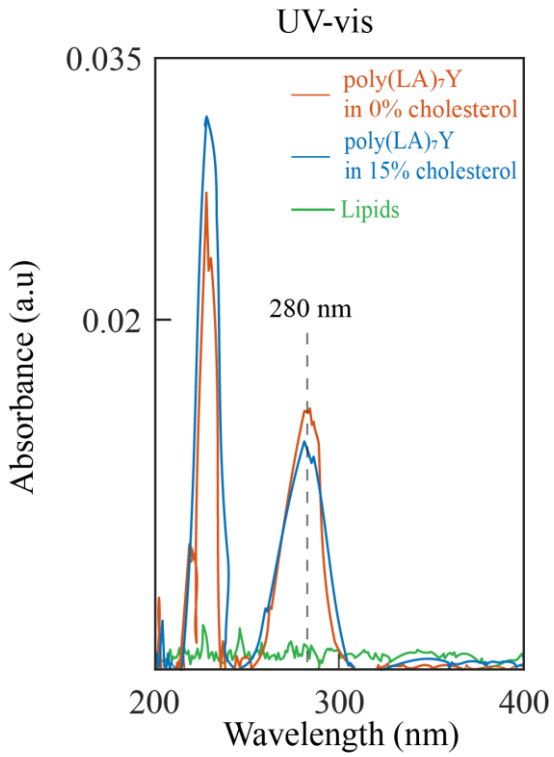

Figure 4.1 Absorption spectrum of tryptophan in poly(LA)$_7$Y. Tryptophan absorbed UV light at 280 nm (red) and with 15% cholesterol weight in DLPG (blue).

To further verify whether this peptide inserted into the liposome, fluorescence measurements were performed. Natural lipoprotein features amphipathicity, and tryptophan fluorescence modes are environmentally sensitive. This can be used to

monitor hydrophobic environments.[21,22] In fluorescence, the peptide poly(LA)$_7$Y, with a tryptophan residue on the c-terminus in aqueous solution indicated a maximum emission wavelength at 362 nm as shown in Figure 4.2A. A slight blue shift was observed in Figure 4.2 B and this tryptophan feature is due to peptide insertion for both the peptide containing the liposome and with 15% cholesterol by weight with peptide in the liposome.

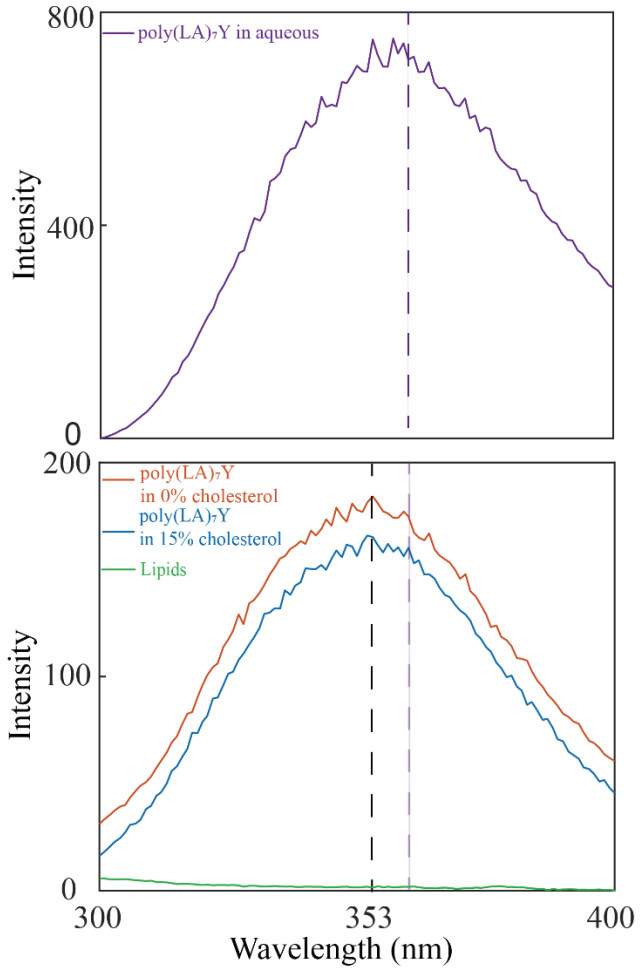

Figure 4.2 (A) Fluorescence of tryptophan in poly(LA)$_7$Y. λ_{ex}=280 nm, λ_{em}=362 nm in aqueous environment. (B) Fluorescence of tryptophan in poly(LA)$_7$Y. λ_{ex}=280 nm, λ_{em}=353 nm in liposome (red), tryptophan in poly(LA)$_7$Y with 15% cholesterol by weight in DLPG (blue), and liposome only (green).

4.3.2 Investigation of Peptide Conformation Using Circular Dichroism (CD) Spectroscopy

Circular dichroism was used to investigate peptide conformation in this study. In principle, left and right circularly polarized light were measured by differential absorbance. In other words, a molecule absorbs left and right circularly polarized light. If molecules are asymmetric and optically active, then the differential absorbance are measured.[23,24,25] The CD data records the ellipticity (θ) in measurement of peptide conformation, since linearly polarized light passes a circular dichroic sample eventually becoming elliptically polarized. In this study, the recorded ellipticity (θ) was converted to mean residue ellipticity (θ_{MRE}) in ($deg \cdot cm^2 \cdot dmol^{-1}$) with following equation,

$$\theta_{MRE} = \frac{\theta}{10 \cdot c \cdot n \cdot l} \tag{4.2}$$

where θ is the ellipticity in mdeg, c is peptide concentration in M, n is the number of peptide bonds, and l is the pathlength in cm. The CD spectra for peptide poly$(LA)_7$ indicated positive ellipticity at 193 nm, and negative ellipticity at 222 nm and 208 nm as shown in Figure 4.3. This figure reveals that the peptide in mimetic lipoprotein model are predominantly α-helices.

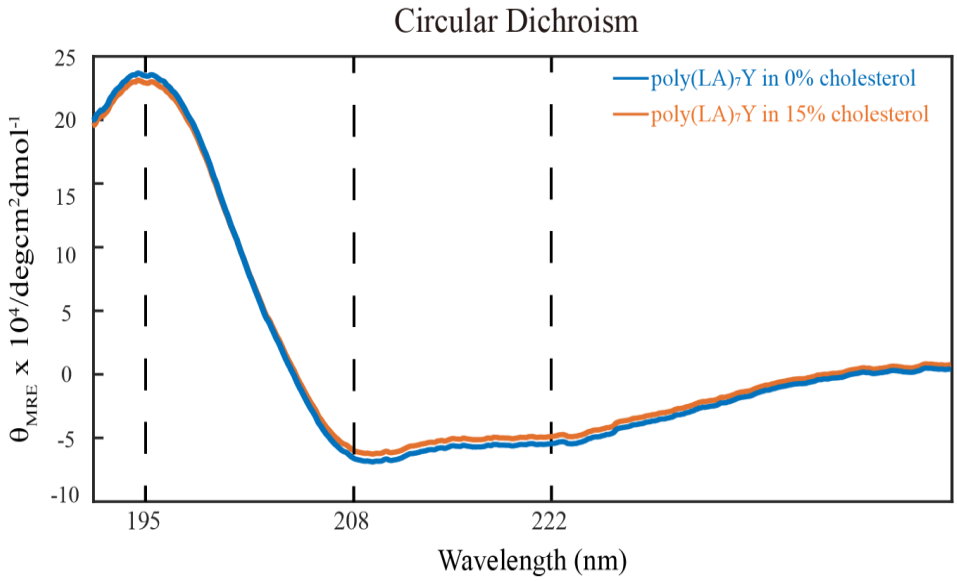

Figure 4.3 CD spectra of peptide with cholesterol weight percent in liposome.

4.3.3 Identification of Mimetic Lipoprotein models Using dUVRR

Raman spectroscopy was used to characterized our mimetic lipoproteins with cholesterol and without cholesterol and peptide as summarized in Figure 4.4. Both spectra are normalized using the same intensity at 930 cm^{-1}. The phosphate buffer and perchlorate peak are subtracted in Figure 4.4B. The excitation wavelength of all components at 197 nm. The unsaturated phospholipids DOPG and saturated DLPC were mixed more likely to simulate natural phospholipids on the shell of a lipoprotein.

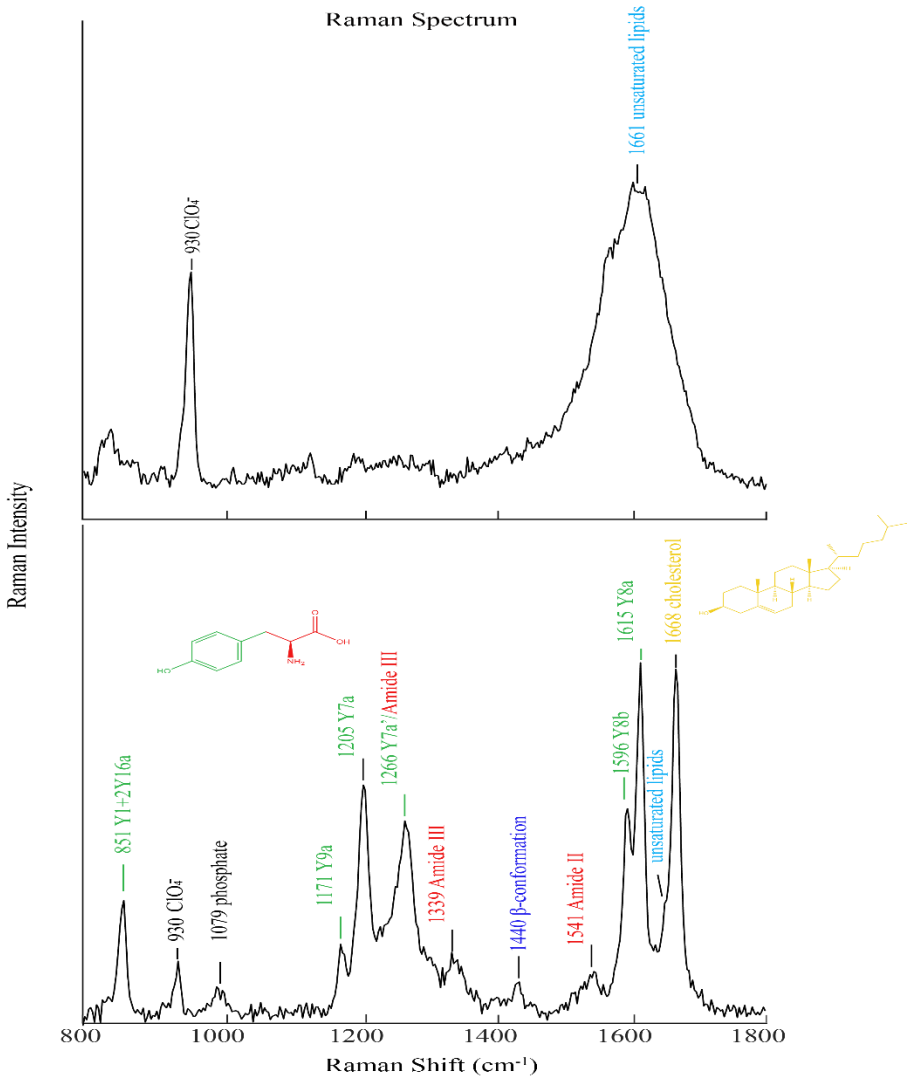

Figure 4.4 (A) Raman spectra of phospholipids (B) 15% of cholesterol with peptide in liposome.

The main peak for phospholipids was measured in a broad peak near 1661 cm^{-1} (Figure 4.4A). The phospholipids intensity depends on percentage of cholesterol (at 1675 cm^{-1}) added. The intensity of the phospholipids peak decreased compared to cholesterol and without cholesterol that was observed in Figure 4.4. This effect resulted from self-

absorption of cholesterol in the Raman scattering. In addition, the ratio of two peaks intensity shifted when changed cholesterol level but this study didn't present this change. The amide I region is dominated by C=C double bonds for unsaturated lipids and cholesterol and is observed from 1600 to 1675 cm^{-1}. The saturated lipids do not possess this feature in this region.[26,27] The amide II band (1541 cm^{-1}) indicates α-helical conformations of the peptide. In addition, the peptide backbone designated out of phase combination of in-plane N-H bending and C-N stretch enhancing intensity is observed in this region. The amide S region and Amide III regions generally represent disordered structure of peptides, but this spectrum shows minimal effects of a disordered structure. The Amide III band contains an intense peak at 1266 cm^{-1} and is likely due to the tyrosine ring-O mode.[28] The Table 4.1 summarized the features of tyrosine at 851, 1171, 1205, 1596, and 1615 cm^{-1}, respectively as well as including other component cholesterol and amide modes. The Small portion of β-conformation appeared at 1440 cm^{-1}. This could be possible due to alanine rich peptide in poly$(LA)_7Y$.[29] In addition, Figure 4.4 contains features for the POH bending of phosphate ion present in the phosphate buffer at 1079 cm^{-1}. It may due incomplete subtraction of phosphate buffer blank.[30] Interestingly, we found that the tryptophan signal was suppressed using an excitation wavelength of 197 nm and may be attributed to the aromatic side chain.[31]

Table 4.1 Summary of bands in Raman spectra for mimetic lipoprotein

Assignment	Designation	Vibrational Mode	Raman Shift (cm^{-1})
Tyrosine	Y8a	ring stretch	1615
Tyrosine	Y8a	ring stretch	1596
β-conformation	L&A	Cα-H bend of β-sheet	1440
Tyrosine	Y7a'	CO stretch	1266
Tyrosine	Y7a	CC stretch	1205
Tyrosine	Y9a	CC stretch	1171
Tyrosine	Y1+2Y16a	Fermi doulet	851 and 830
Amide backbone	Amide III	CN stretch + NH bend	1266 and 1339
Amide backbone	Amide II	CN stretch + NH bend	1541
Unsaturated lipids	DOPG	N/A	1661
Cholesterol	Cholesterol	N/A	1668

4.4 Conclusion

This study provided a view of the characterization of mimetic lipoprotein models using deep-UV-Vis Resonant Raman spectroscopy. This technique enhanced the signals from the backbone of tyrosine as a C-terminus inserted in liposomes and also gave a clear fingerprint region for cholesterol content in the mimetic environment. Circular dichroism provided view of secondary structure of peptide poly$(LA)_7$Y to confirm peptide conformation. UV-Vis and fluorescence spectroscopy identified peptide and verified insertion in the liposome. These studies provide further support of the mimetic lipoprotein model.

4.5 Reference

1. Virani, S. S.; Alonso, A.; Benjamin, E. J.; Bittencourt, M. S.; Callaway, C. W.; Carson, A. P.; Chamberlain, A. M.; Chang, A. R.; Cheng, S.; Delling, F. N.; Djousse, L.; Elkind, M. S. V.; Ferguson, J. F.; Fornage, M.; Khan, S. S.; Kissela, B. M.; Knutson, K. L.; Kwan, T. W.; Lackland, D. T.; Lewis, T. T.; Lichtman, J. H.; Longenecker, C. T.; Loop, M. S.; Lutsey, P. L.; Martin, S. S.; Matsushita, K.; Moran, A. E.; Mussolino, M. E.; Perak, A. M.; Rosamond, W. D.; Roth, G. A.; Sampson, U. K. A.; Satou, G. M.; Schroeder, E. B.; Shah, S. H.; Shay, C. M.; Spartano, N. L.; Stokes, A.; Tirschwell, D. L.; VanWagner, L. B.; Tsao, C. W.; *Circulation* **2020**, *141*, e139–e596.
2. Castelli, W. P.; Garrison, R. J.; Wilson, P. W. F.; Abbott, R. D.; Kalousdian, S.; Kannel, W. B. *JAMA* **1986**, *256*, 2835–2838.
3. Mudd, J. O.; Borlaug, B. A.; Johnston, P. V.; Kral, B. G.; Rouf, R.; Blumenthal, R. S.; Kwiterovich, P. O. J. Am. Coll. Cardiol. **2007**, *50* (18), 1735–1741.
4. Grundy, S. M.; Cleeman, J. I.; Daniels, S. R.; Donato, K. A.; Eckel, R. H.; Franklin, B. A.; Gordon, D. J.; Krauss, R. M.; Savage, P. J.; Smith, S. C.; Spertus, J. A.; Costa, F. *Circulation* **2005**, *112* (17), 2735–2752.
5. Cleeman, J.; Grundy, S.; Becker, D.; Clark, L.; Cooper, R.; Denke, M.; Howard, W.; Hunninghake, D.; Illingworth, D.; Luepker, R.; McBride, P.; McKenney, J.; Pasternak, R.; Stone, N.; Van Horn, L.; Brewer, H.; Ernst, N.; Gordon, D.; Levy, D.; Rifkind, B.; Rossouw, J.; Savage, P.; Haffner, S.; Orloff, D.; Proschan, M.; Schwartz, J.; Sempos, C.; Shero, S.; Murray, E. *JAMA.* **2001**, *285*, 2486–2497.

6. Miller, W. G.; Myers, G. L.; Sakurabayashi, I.; Bachmann, L. M.; Caudill, S. P.; Dziekonski, A.; Edwards, S.; Kimberly, M. M.; Korzun, W. J.; Leary, E. T.; Nakajima, K.; Nakamura, M.; Nilsson, G.; Shamburek, R. D.; Vetrovec, G. W.; Warnick, G. R.; Remaley, A. T. *Clin. Chem.* **2010**, *56* (6), 977–986.

7. Chapman, M. J.; Goldstein, S.; Lagrange, D.; Laplaud, P. M. *J Lipid Res.* **1981**, *22* (2), 339–358.

8. Asztalos, B. F.; Collins, D.; Horvath, K. V.; Bloomfield, H. E.; Robins, S. J.; Schaefer, E. J. *Metabolism*. **2008**, *57* (1), 77–83.

9. Rainwater, D.; Andres, D.; Ford, A.; Lowe, F.; Blanche, P.; Krauss, R.. *J Lipid Res.* **1992**, *33* (12), 1876–1881.

10. Collins, L. A.; Mirza, S. P.; Kissebah, A. H.; Olivier, M. *Physiol Genomics*. **2010**, *40* (3), 208–215.

11. de la Llera Moya, M.; McGillicuddy, F. C.; Hinkle, C. C.; Byrne, M.; Joshi, M. R.; Nguyen, V.; Tabita-Martinez, J.; Wolfe, M. L.; Badellino, K.; Pruscino, L.; Mehta, N. N.; Asztalos, B. F.; Reilly, M. P. *Atherosclerosis* **2012**, *222* (2), 390–394.

12. Rosenson, R. S.; Brewer, H. B.; Ansell, B.; Barter, P.; Chapman, M. J.; Heinecke, J. W.; Kontush, A.; Tall, A. R.; Webb, N. R. *Circulation*. **2013**, *128* (11), 1256–1267.

13. Harz, M.; Claus, R. A.; Bockmeyer, C. L.; Baum, M.; Rösch, P.; Kentouche, K.; Deigner, H.-P.; Popp, J. *Biopolymers* **2006**, *82* (4), 317–324.

14. Harz, M.; Bockmeyer, C. L.; Rösch, P.; Claus, R. A.; Popp, J. *Med Laser Appl*. **2007**, *22* (2), 87–93.

15. Atkins, C. G.; Buckley, K.; Blades, M. W.; Turner, R. F. B. *Appl Spectrosc* **2017**, *71* (5), 767–793.

16. Bricarello, D. A.; Smilowitz, J. T.; Zivkovic, A. M.; German, J. B.; Parikh, A. N. *ACS nano* **2011**, *5* (1), 42–57.

17. Balakrishnan, G.; Spiro, T. G. Ultraviolet Resonance Raman (UVRR) Spectroscopy Studies of Structure and Dynamics of Proteins. In *Encyclopedia of Biophysics*; Roberts, G. C. K., Ed.; Springer Berlin Heidelberg: Berlin, Heidelberg, 2013; pp 2697–2707.

18. Krimm, S., and Bandekar, J. Vibrational spectroscopy and conformation of peptides, polypeptides and proteins, In *Advances in Protein Chemistry;* Anfinson, C. B., Edsall, J. T., and Richards, F. M., Eds.; 1986; pp 181-365, Academic Press, New York.

19. Wang, Y.; Purrello, R.; Jordan, T.; Spiro, T. G. *J. Am. Chem. Soc.* **1991**, *113* (17), 6359–6368.

20. Chi, Z.; Chen, X. G.; Holtz, J. S. W.; Asher, S. A. *Biochemistry* **1998**, *37* (9), 2854–2864.

21. Vivian, J. T.; Callis, P. R. *Biophys. J.* 2001, 80, 2093–2109.

22. Ladokhin, A. S.; Jayasinghe, S.; White, S. H. *Anal. Biochem.* **2000**, *285* (2), 235–245.

23. Greenfield, N. J. *Nat Protoc*. **2006**, *1* (6), 2876–2890.

24. Webb, R. L. Circular Dichroism. Principles and Applications, Second Edition Edited by Nina Berova, Koji Nakanishi, and Robert W. Woody. Wiley-VCH Publishers, New York, 2000.

25. Archer, R. D. Inorganic Electronic Structure and Spectroscopy. Volume II. Applications and Case Studies Edited by Edward I. Solomon (Stanford University) and A. B. P. (Barry) Lever (York University). Wiley-Interscience: New York. 1999.

26. Halsey, C. M.; Benham, D. A.; JiJi, R. D.; Cooley, J. W. *Spectrochimica Acta Part A: Molecular and Biomolecular Spectroscopy* **2012**, *96*, 200–206.

27. Eagleburger, M. K.; Cooley, J. W.; JiJi, R. D. *Biopolymers* **2014**, *101* (8), 895–902.

28. Fodor, S. P. A.; Copeland, R. A.; Grygon, C. A.; Spiro, T. G. *J. Am. Chem. Soc.* **1989**, *111* (15), 5509–5518.

29. Shi, Z.; Olson, C. A.; Rose, G. D.; Baldwin, R. L.; Kallenbach, N. R. *Proc. Natl. Acad. Sci.* U.S.A. **2002**, *99*, 9190.

30. Sosa Morales, M. C.; Álvarez, R. M. S. *J Raman Spec*. **2017**, *48* (2), 170–179.

31. Huang, C.-Y.; Balakrishnan, G.; Spiro, T. G. *J Raman Spec*. **2006**, *37* (1–3), 277–282.

Chapter 5: Future Directions and Extensions

5.1 Establish mimetic lipoprotein standards to explore how lipoproteins relate to CVD

Studies of cardiovascular disease (CVD) have tried to relate age, sex, history of alcohol or smoking, and generic factors as ways to monitor the disease. Lipoproteins studies have tried to determine their role in cardiovascular disease for decades. Research has focused on various properties of lipoproteins such as the size of lipoproteins, lipoprotein content, and its metabolic pathways as way to understand CVD. Many methods have been developed to assess lipoproteins. For example, the most common method used is ultracentrifugation to separate lipoproteins based on densities.[1] In addition, gel electrophoresis, based on electrophoretic mobility, has been used to measure the apolipoprotein content of lipoproteins.[2] HPLC methods have been developed to investigate lipoproteins based mostly on their size or apoprotein charge.[3,4,5] In previous lipoprotein chapters, a new method was introduced to provide a spectroscopic characterization of mimetic lipoprotein models. The combination of UV-Vis, fluorescence, circular dichroism, dynamic light scattering, and dUVRR spectroscopy investigated mimetic lipoprotein models. These techniques provided additional information of cholesterol content, putative apoproteins (a lab synthesized peptide) and phospholipids. These components in native lipoproteins have been associated with cardiovascular disease.[6,7,8] In previous unpublished data from my group, we found that HDL, LDL, and VLDL can be characterized by Raman spectroscopy. Figure 5.1 shows three representative lipoprotein classes. Main cholesterol peaks were observed in each individual lipoprotein spectra at 1675 cm^{-1}. The tyrosine/Amide III region was observed

using an excitation wavelength of 197 nm. For blood serum lipoproteins, some information was discerned. The Friedewald equation or Red Amplex Assay can be used to measure cholesterol content and provide total concentrations of cholesterol in LDL. Presumably, the cholesterol content was high, but there was little LDL in sample. These latter two methods have issues when trying to measure the cholesterol content and distinguish between sample with a high cholesterol content in low amounts of lipoproteins versus low cholesterol content in the presence of high lipoprotein concentrations.

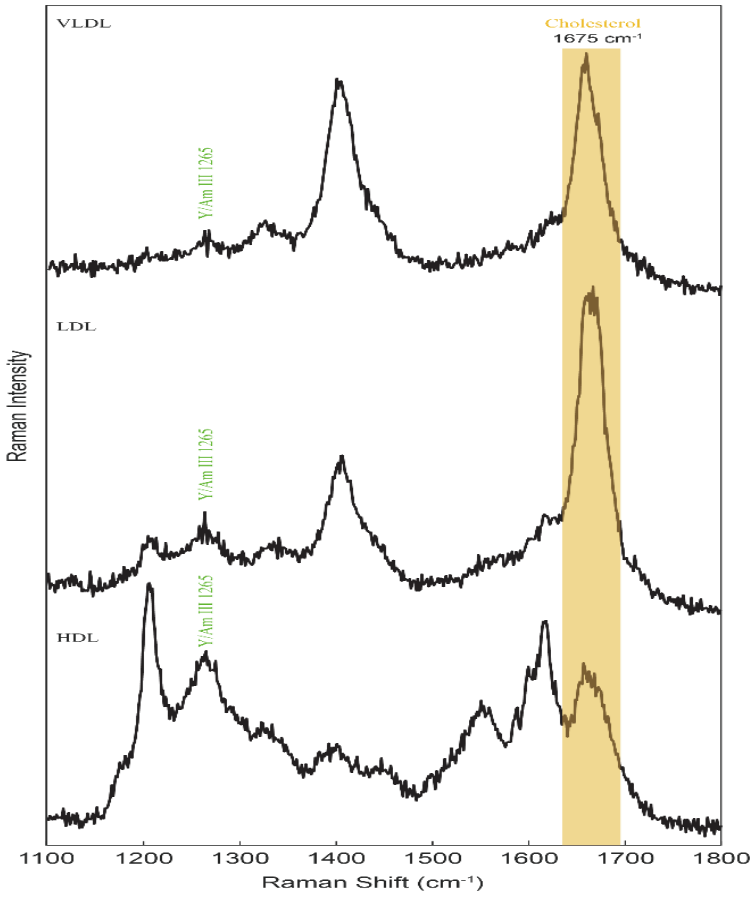

Figure 5.1 Representative Raman spectra of VLDL (top), LDL (middle), and HDL (bottom) from blood serum. Courtesy of Dr. Michael Eagleburger

An extension of this study should continue to develop mimetic lipoprotein models with additional cholesterol contents. Mimetic lipoprotein standards combined with MCR-ALS (multivariate curve resolution-alternating least square), recovering pure component profiles from complex structure and environment, can be applied as a quantitative tool in complex samples. This algorithm analysis can be applied in hyperspectral images. In mathematical terms, the MCR-ALS is written as,

$$D = CS^T + E \tag{5.1}$$

where D is a matrix containing spectra of all pixels of images, C and S^T represent concentration profiles and pure spectral. E is matrix of experimental error. In future studies, each pure concentration or pure spectral profiles from mimetic models will input along with serum samples to provide predictions of cholesterol, or other components level in the lipoproteins. This process is depicted in Figure 5.2. The concentration profiles, term C, can be achieved by applying size exclusion chromatography from both serum lipoprotein and individual component from mimetic lipoproteins. S^T can be determined with dUVRR spectroscopy. MCR-ALS has the advantage of a non-negativity constraint to provide minimal interference in quantitative analysis.

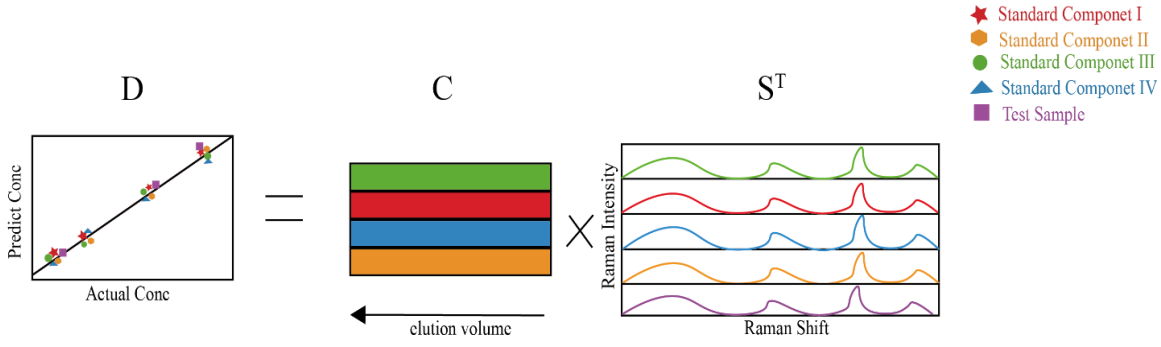

Figure 5.2 Schematic of MCR-ALS Analysis.

5.2 Exploration of NNAL and NNAL-Glucs in human toenails

NNAL 4-(methylnitrosamino)-1-(3-pyridyl)-1-butanol and NNAL-Glucs (glucuronides) have played significant roles in biomarker research in lung cancer studies. NNK nitrosamine 4-(methylnitrosamino)-1-(3-pyridyl)-1-butanone is major constituent in tobacco and also acts as a precursor for NNAL and NNAL-Glucs. In early studies, NNK was found to lead to lung carcinogenesis and caused tumor growth in other organs in rats and hamsters.[9,10] There are also studies in human research on metabolites of NNK, NNAL and NNAL-Glucs, in urine and blood samples from those exposed to secondhand smoke and smokers, including quantitative analysis of NNAL and NNAL-Glucs.[11,12] These are invasive samples and sample preparation was often labor intensive. In addition, most common way of obtaining NNAL and NNAL-Glucs is to apply solid phase extractions with one or more cartridges required, e.g. Chem-Elut and Oasis MCX or equivalent. Quantitative analysis of nicotine was investigated in this work by applying liquid-liquid extractions prior to HPLC-MS analysis. Human toenails samples were used to measure nicotine levels. Toenails exhibit long term accumulation of nicotine and other metabolites from exposure to tobacco and are stable storage at ambient. NNAL and NNAL-Glucs from NNK are only 7% to 9% in total body fluids. Thus, toenails are suitable candidates in research of NNAL and NNAL-Gluc[13]. However, nicotine level determined were only based on population between healthy non-smokers exposed to secondhand smoke and smokers. NNAL and NNAL-Glucs are excellent biomarkers in lung cancer. Further investigation of NNAL and NNAL-Glucs in lung cancer studies with toenails can be extended to large studies exploring factors such as age, race, and sex. Age and sex may play minor factors in analysis of NNAL and NNAL-Glucs, but race may

play a bigger factor. In human lungs, European, Asians and African Americans have different genes in CHRNA5-CHRNA3-CHRNB4 region, these gene regions are associated with smoking and non-smoking. People carrying the CHRNA5 and CHRNA3 gene have higher NNAL levels with a higher risk of lung cancer[14]. In addition, NNAL-Glucs is considered non-carcinogenic and likely to be detoxification products. Thus, future studies may also be interested in the investigation of the levels of NNAL-Glucs and their role in regulating liver enzymes. In the analysis of NNAL and NNAL-Glucs, QuECHERS (Quick, Easy, Cheap, Rugged, Safe) methods can be developed to simplify sample extractions. This method is low cost and non-toxic, and gives high selectivity and high recovery. This extraction method is similar to that used in a study of hair, which is another type of a keratinic matrix.[15] Continuing investigations of human toenails with HPLC-MS, extended to a large cohort study would also be beneficial.

5.3 Reference

1. Havel, R. J.; Eder, H. A.; Bragdon, J. H. *J. Clin. Invest.* **1955**, *34* (9), 1345–1353.

2. Noble, R. P.; Hatch, F. T.; Marzimas, J. A.; Lindgren, F. T.; Jensen, L. C.; Adamson, G. L. *Lipids* **1969**, *4* (1), 55–59.

3. Hara, I.; Okazaki, M. High-Performance Liquid Chromatography of Serum Lipoproteins. In *Methods in Enzymology*; Academic Press, 1986; Vol. 129, pp 57–78.

4. Okazaki, M.; Usui, S.; Ishigami, M.; Sakai, N.; Nakamura, T.; Matsuzawa, Y.; Yamashita, S. *Arterioscler. Thromb. Vasc. Biol.* **2005**, *25* (3), 578–584.

5. Usui, S.; Hara, Y.; Hosaki, S.; Okazaki, M. *J. Lipid Res.* **2002**, *43* (5), 805–814.

6. Sniderman, A. D.; Dagenais, G. R.; Cantin, B.; Després, J.-P.; Lamarche, B. *Am. J. Cardiol.* **2001**, *87* (6), 792–793, A8.

7. Nordestgaard, B. G.; Chapman, M. J.; Ray, K.; Borén, J.; Andreotti, F.; Watts, G. F.; Ginsberg, H.; Amarenco, P.; Catapano, A.; Descamps, O. S. *Eur. Heart J.* **2010**, *31* (23), 2844–2853.

8. Bachorik, P. S.; Cloey, T. A.; Finney, C. A.; Lowry, D. R.; Becker, D. M. *Ann. Intern. Med.* **1991**, *114* (9), 741–747.

9. Hecht, S. S. *Chem. Res. Toxicol.* **1998**, *11* (6), 559–603.

10. Hecht, S. S.; Rivenson, A.; Braley, J.; DiBello, J.; Adams, J. D.; Hoffmann, D. *Cancer Res.* **1986**, *46* (8), 4162.

11. Carmella, S. G.; Han, S.; Villalta, P. W.; Hecht, S. S. *Cancer Epidemiol. Biomark. Amp Prev.* **2005**, *14* (11), 2669.

12. Hecht, S. S.; Carmella, S. G.; Ye, M.; Le, K.; Jensen, J. A.; Zimmerman, C. L.; Hatsukami, D. K. *Cancer Res.* **2002**, *62* (1), 129.

13. Benowitz, N. L.; Hukkanen, J.; Jacob, P. *Handb. Exp. Pharmacol.* **2009**, No. 192, 29–60.

14. Hecht, S. S.; Yuan, J.-M.; Hatsukami, D. *Chem. Res. Toxicol.* **2010**, *23* (6), 1001–1008.

15. Kim, J.; Cho, H.-D.; Suh, J. H.; Lee, J.-Y.; Lee, E.; Jin, C. H.; Wang, Y.; Cha, S.; Im, H.; Han, S. B. *Molecules* **2020**, *25* (8). https://doi.org/10.3390/molecules25081763.

APPENDIX 1: List of abbreviations

A	Alanine
ACN	Acetonitrile
ApoB	Apolipoprotein B
CAD	Cardiovascular artery disease
CCD camera	Charged couple device camera
CD	Circular Dichroism spectroscopy
CE-SDS	Capillary electrophoresis sodium dodecyl sulfate
CHRNA3	Cholinergic Receptor Nicotinic Alpha 3 Subunit
CHRNA4	Cholinergic Receptor Nicotinic Beta 4 Subunit
CHRNA5	Cholinergic Receptor Nicotinic Alpha 5 Subunit
CID	Collision induced dissociation
CVD	Cardiovascular disease
DLPC	1,2-dilauroyl-sn-glycero-3-phosphocholine
DLS	Dynamic light scattering spectroscopy
DOPG	1,2-dioleoyl-sn-glycero-3-phospho-(1'-rac-glycerol
DPH	1,6-diphenyl-1,3,5-hexatriene
dUVRRS	Deep UV-vis resonance Raman spectroscopy
ELISA	enzyme-lined immunoassay
ESI	Electrospray ionization
GC-ECD	Gas chromatography electron capture detector
GC-MS	Gas chromatography mass spectrometry

HDL	High density lipoproteins
HFIP	1,1,1,3,3,3-hexafluoro-2-propanol
HOMA-IR	Homeostasis model assessment insulin resistance
HPLC	High performance liquid chromatography
HPLC-ECD	High performance liquid chromatography-Electrochemical detector
HPLC-GPC	High performance liquid chromatography gel permeation column
IDL	Intermediate density lipoproteins
K	Lysine
L	Leucine
LC-MS/MS	Liquid chromatography Mass spectrometry
LDL	Low density lipoproteins
LOD	Limit of Detection
LOQ	Limit of Quantitation
m/z	Mass to ration
ME	Matrix Effect
MCR-ALS	Multivariate curve resolution-alternating least square
MEPS	Microextraction by packed sorbent
ND-PAGGE	Non-denaturant polyacrylamide gradient gel electrophoresis
Nicotine-d_3	Deuterated nicotine
NMR	Nuclear magnetic resonance
NNAL	4-(methylnitrosamino)-1-(3-pyridyl)-1-butanol
NNAL-Gluc	4-(methylnitrosamino)-1-(3-pyridyl)-1-butanol-glucuronides
NNK	4-(methylnitrosamino)-1-(3-pyridyl)-1-butanone

Oasis-MCX	Oasis mixed mode cation exchange
QuECHERS	Quick, Easy, Cheap, Rugged, and Safe
RE	Recovery
RIA	Radioimmunoassay
RSD	Relative standard deviation
SPE	Solid phase extraction
UV-vis	Ultraviolet visible spectroscopy
VLDL	Very low density lipoproteins
W	Tryptophan
WHO	World Health Organization
Y	Tyrosine
2D-PAGGE	Two-dimensional polyacrylamide gradient gel electrophoresis

APPENDIX 2: Chapter 2-Solid phase extraction Calibration Curve

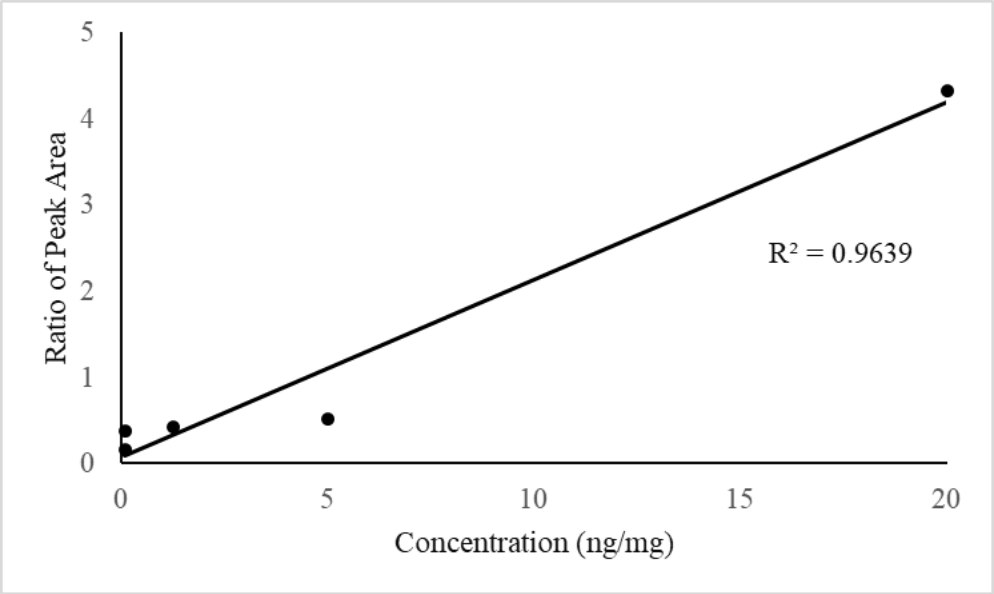

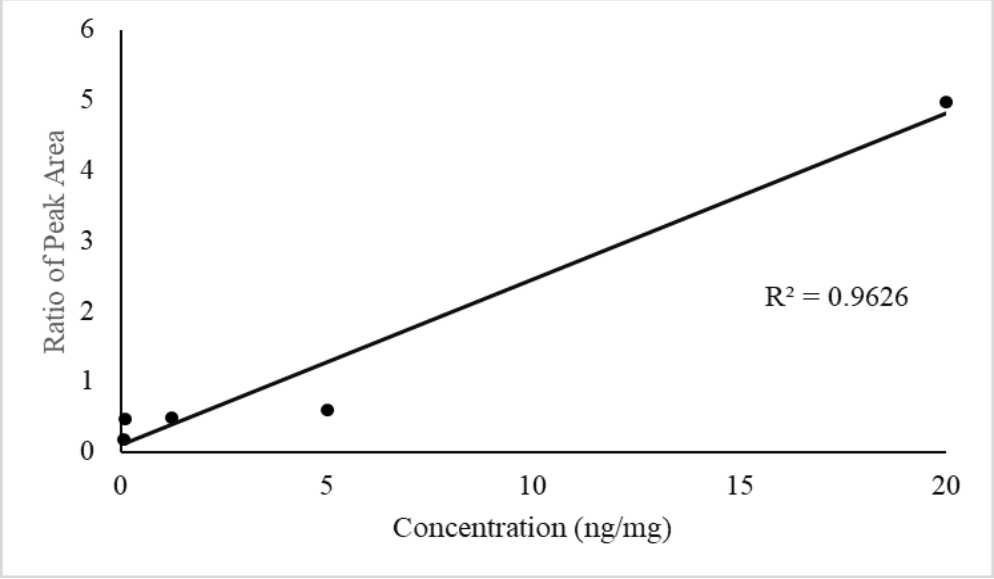

Figure A2.1. Nicotine calibration curves using the two major fragmentation ions at (A) m/z 132 and (B) m/z 106 in method of solid phase extraction.

APPENDIX 3: Chapter 3-Dynamic Light Scattering Measurement of Radius

Table A3.1. The radius, poly dispersity and poly dispersity index (PDI) of DLPG and DOPG liposomes suspended in PBS were obtained for 20 scans using dynamic light scattering (DLS). The mean radius and standard deviation (SD) for all scans are also included.

#	Radius (nm)	Poly dispersity (nm)	Poly dispersity index
1	41.7	37.9	0.75
2	38.9	31.7	0.66
3	42.2	34.6	0.67
4	39.8	28.2	0.5
5	42.2	39.3	0.69
6	41.5	39.4	0.9
7	37.6	25.6	0.44
8	42.2	30.8	0.53
9	40.6	31.4	0.6
10	42.4	40.5	0.91
11	40.3	30.2	0.53
12	38.8	31.5	0.66
13	40	33.6	0.58
14	37.9	25.6	0.43
15	40	35.3	0.67
16	41.1	38.8	0.81
17	40.5	40.1	0.81
18	40.8	31.4	0.56
19	40.2	26.1	0.36
20	40.9	37	0.68
Mean	40.5	33.5	0.6
SD	1.4	4.8	0.1

APPENDIX 4: Chapter 4-Circular Dichroism of Ovalbumin Conformation Spectra

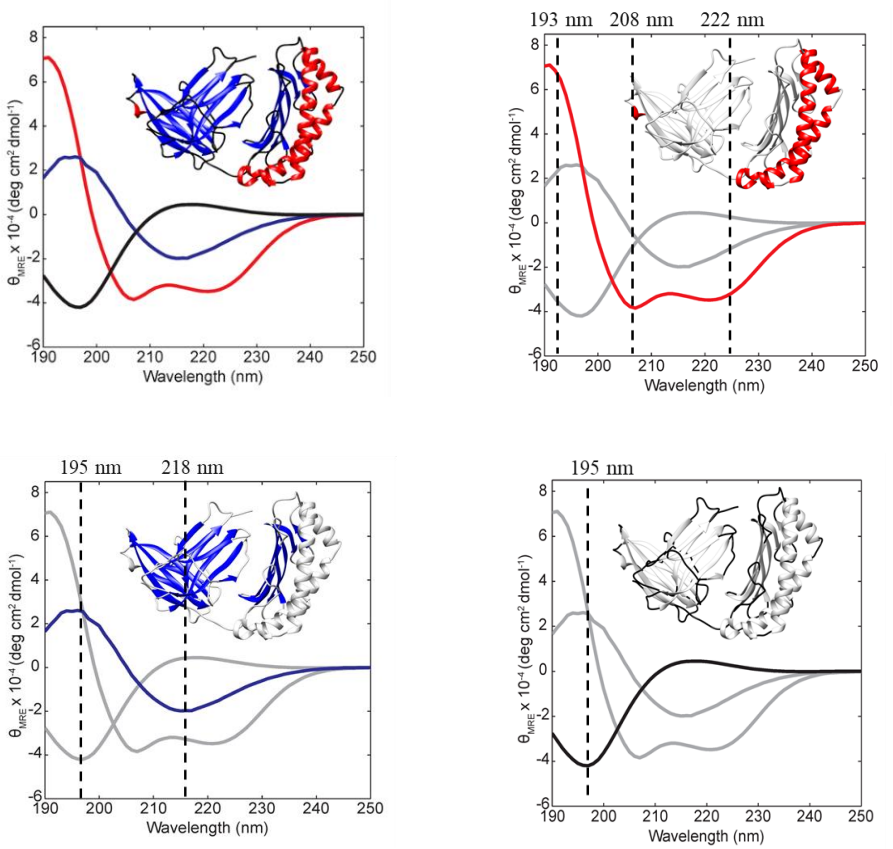

FigureA4. 1. Ovalbumin CD spectrum for secondary structure (top left), α-helix (top right), β-sheet (bottom left), and disorder form (bottom right). Courtesy of Dr. Jian Xiong.

VITA

Xiyang Li grew up in the city of Kunming, Yunnan Province, China. He came to the United States in 2011 and obtained Bachelor of Science degree majoring in Chemistry-Prepharmacy with a minor in biology at Ohio University-Athens. He worked with Dr. Hao Chen in the analytical chemistry division at Ohio University for a short period time of post-graduation in 2015.

Xiyang began new journey with his graduate studies in analytical chemistry pursuing PhD degree at the University of Missouri-Columbia in 2016. He worked with Dr. JiJi Renee with focusing on characterization lipoproteins and its mimicking models when he was first- and second-year graduate student in Chemistry Department. He joined Dr. Michael Greenlief's research group in 2018. Under Dr. Greenlief's supervision, Xiyang focused on quantitative analysis using high performance liquid chromatography coupled with mass spectrometry in nicotine analysis for human toenails. He developed analytical method and applied the method to extract and analyze nicotine from human toenails in secondhand smoke. Xiyang had opportunities to serve as a teaching assistant and president of Chinese students and scholars association while he was at the University of Missouri-Columbia. He graduated from the University of Missouri-Columbia with a PhD. in analytical chemistry in December 2021.

Xiyang accepted staff scientist position at Eurofins in Columbia, Missouri, beginning in August 2021. He joined the Biotech Department within the Biochemistry Division. He has contributed his knowledge of quantitative analysis and analytical instruments while working at Eurofins.